Science of the Total Environment 857 (2023) 159386

Contents lists available at ScienceDirect

Science of the Total Environment

journal homepage: www.elsevier.com/locate/scitotenv

Discovering oxidative potential (OP) drivers of atmospheric PM_{10}, $PM_{2.5}$, and PM_1 simultaneously in North-Eastern Spain

Marten in 't Veld [a,b,*], M. Pandolfi [a], F. Amato [a], N. Pérez [a], C. Reche [a], P. Dominutti [c], J. Jaffrezo [c], A. Alastuey [a], X. Querol [a], G. Uzu [c]

[a] Institute of Environmental Assessment and Water Research, IDAEA-CSIC, Barcelona 08034, Spain
[b] Department of Civil and Environmental Engineering, Universitat Politècnica de Catalunya, Barcelona 08034, Spain
[c] University Grenoble Alpes, CNRS, IRD, INP-G, IGE (UMR 5001), 38000 Grenoble, France

HIGHLIGHTS

- First paper quantifying a yearlong dataset on OP in PM_{10}, $PM_{2.5}$, and PM_1
- Drivers of OP in PM_{10} and PM_1 in the urban station and PM_1 in the rural station
- Multisite multisize PMF identified 9 common sources.
- Main drivers in Barcelona were from Anthropogenic sources.
- PM_1 in Barcelona has different sources driving OP compared to PM_{10} and $PM_{2.5}$.

GRAPHICAL ABSTRACT

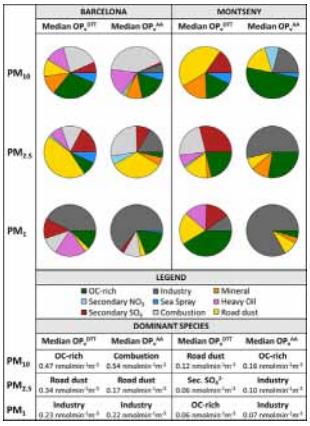

ARTICLE INFO

Editor: Pavlos Kassomenos

Keywords:
Oxidative potential
Source apportionment
Positive matrix factorization
PM_{10}
$PM_{2.5}$
PM_1

ABSTRACT

Ambient particulate matter (PM) is a major contributor to air pollution, leading to adverse health effects on the human population. It has been suggested that the oxidative potential (OP, as a tracer of oxidative stress) of PM is a possible determinant of its health impact. In this study, samples of PM_{10}, $PM_{2.5}$, and PM_1 were collected roughly every four days from January 2018 until March 2019 at a Barcelona urban background site and Montseny rural background site in northeastern Spain. We determined the chemical composition of samples, allowing us to perform source apportionment using positive matrix factorization. The OP of PM was determined by measuring reactive oxygen species using dithiothreitol and ascorbic acid assays. Finally, to link the sources with the measured OP, both a Pearson's correlation and a multiple linear regression model were applied to the dataset. The results showed that in Barcelona, the OP of PM_{10} was much higher than those of $PM_{2.5}$ and PM_1, whereas in Montseny results for all PM sizes were in the same range, but significantly lower than in Barcelona. In Barcelona, several anthropogenic sources were the main drivers of OP in PM_{10} (Combustion + Road Dust + Heavy Oil + OC-rich) and $PM_{2.5}$ (Road Dust + Combustion). In contrast, PM_1 -associated OP was driven by Industry, with a much lower contribution to PM_{10} and $PM_{2.5}$ mass. Meanwhile, Montseny exhibited no clear drivers for OP evolution, likely explaining the lack of a significant difference in OP between PM_{10}, $PM_{2.5}$, and PM_1. Overall, this study indicates that size fraction matters for OP, as a function of the environment typology. In an urban context, OP is driven by the PM_{10} and PM_1 size fractions, whereas only the PM_1 fraction is involved in rural environments.

* Corresponding author at: Institute of Environmental Assessment and Water Research, IDAEA-CSIC, Barcelona 08034, Spain.
E-mail address: Marten.Veld@idaea.csic.es (M. in 't Veld).

http://dx.doi.org/10.1016/j.scitotenv.2022.159386
Received 10 August 2022; Received in revised form 23 September 2022; Accepted 8 October 2022
Available online 12 October 2022

1. Introduction

Ambient particulate matter (PM) is a major contributor to air pollution, causing several detrimental effects on health, ecosystems, and climate (Apte et al., 2015; Cohen et al., 2017; Jacob, 1999; Lelieveld et al., 2015, 2020). PM has known negative effects on human health with both short- and long-term outcomes, such as aggravation of cardiovascular and respiratory symptoms, and development of cancer, among others (WHO, 2021a, 2016; W. Zhang et al., 2018b). The WHO has stated that air pollution is now recognized as the single biggest environmental threat to human health, even updating the air quality guideline levels of PM (WHO, 2021b).

In air quality science, PM is classified by its size, with the most common distinctions being PM_{10} (aerodynamic diameter < 10 μm), $PM_{2.5}$ (< 2.5 μm), PM_1 (< 1 μm), and $PM_{0.1}$ (< 0.1 μm). The particle size of PM affects its uptake route by the human body, as coarser particles (i.e., $PM_{2.5–10}$) can be filtered out before entering the body. In contrast, finer particles ($PM_{2.5}$ or PM_1) can more easily penetrate and enter the respiratory system, and even affect the vascular and nervous systems, as in the case of $PM_{0.1}$ (Nelin et al., 2012; WHO, 2006). Moreover, chemical composition also has a significant influence on the toxicity of PM (Jia et al., 2017; Li et al., 2019). PM consists of a multitude of primary and secondary components, containing variable proportions of carbonaceous species, metals, and salts, depending on the major emission sources (both anthropogenic and natural) that drive the variability of PM levels at a given site (in 't Veld et al., 2021; Jia et al., 2017; Pandolfi et al., 2014; Querol et al., 2004a, 2004b, 2006; H. Zhang et al., 2018a). Changes in chemical composition can lead to a significant difference in the relative toxicity (normalized per unit of concentration) of PM (Jia et al., 2017). Although no clear hierarchy in toxicity of PM components has been currently demonstrated due to the complex structure of PM and its interaction with co-pollutants (WHO, 2013), studies have indicated that organic carbon (very often associated with elemental carbon) and metals such as Fe, Cu, As, Cd, Ni, and V appear to have a larger impact on the toxicity of PM than do other PM components.

(Hime et al., 2018; Kelly and Fussell, 2012; WHO, 2013; W. Zhang et al., 2018b). This can lead to a situation where PM concentrations may have decreased, but the relative toxicity, and therefore hazardous effect, of PM has increased (Hopke and Hidy, 2022). For instance, W. Zhang et al. (2018b) demonstrated that even though cardiovascular hospital admissions attributable to $PM_{2.5}$ have been markedly reduced in parallel to ambient $PM_{2.5}$ abatements, the normalized excess risk rate for this health outcome has increased by a factor of three for $PM_{2.5}$ between the periods of 2005–2007 and 2014–2016. This was speculated to be the result of compositional changes.

To evaluate possible changes in the chemical composition of $PM_{2.5}$ in Barcelona, northeastern Spain (BCN), in 't Veld et al. (2021) performed a $PM_{2.5}$ timeseries study for the period 2009–2018, both for the BCN urban background site and for a close regional background site (Montseny, MSY, also in northeastern Spain). During this period, decreases in $PM_{2.5}$ concentrations of 29 % and 26 % were reported for BCN and MSY, respectively. At the same time, the relative contribution of organic aerosols (OA) was observed to increase by 12 % in BCN and 9 % in MSY. This increase was mostly driven by secondary organic aerosols (SOA), the relative contributions of which increased by 7 % and 4 % in BCN and MSY, respectively, in addition to a relative decrease in secondary inorganic aerosols (sulfate, nitrate, and ammonium; −5 % in BCN and + 1 % in MSY). At the end of the period of study, OA accounted for 40 % and 50 % of the annual mean $PM_{2.5}$ mass in BCN and MSY, respectively. These changes in chemical composition may have potentially led to a change in toxicity patterns of PM, as SOA is linked to hazardous effects on human health (Chowdhury et al., 2019; Decesari et al., 2017; Delfino et al., 2010; Park et al., 2018; W. Zhang et al., 2018b), and is known to be one of the main drivers of the oxidative potential (OP) of PM (Daellenbach et al., 2020).

As previously mentioned, the toxic effects of PM are diverse due to the many possible different chemical and physical characteristics of its components, which increases the complexity of determining those hazardous effects (Jacob, 1999; WHO, 2013, 2018, 2021a). It has been suggested that measuring indicators of the oxidative stress of PM, such as OP, might help to identify some of the many possible drivers of the associated health effects (Daellenbach et al., 2020). Although this link remains subject to relevant uncertainty (Bates et al., 2015; Daellenbach et al., 2020; Weichenthal et al., 2016), it has been applied in a number of studies (e.g., Abbasi et al., 2020; Borlaza et al., 2021a, 2021b; Calas et al., 2018, 2019; Cesari et al., 2019; Charrier et al., 2015; Daellenbach et al., 2020; Gulliver et al., 2018; Janssen et al., 2014; Li et al., 2019; Naraki et al., 2021; Trechera et al., 2021; Wang et al., 2018; Weber et al., 2018, 2019).

The current paper presents results as a continuation of the previous study by in 't Veld et al. (2021). Although In 't Veld et al. (2021) measured an increase in OA, they were unable to determine if this led to a more toxic PM composition. The main goal of this paper is therefore to determine the OP of the PM, and to gain insights regarding which species and source contributions are the main drivers of OP in the study area. To achieve this goal, a chemical speciation of PM_{10}, $PM_{2.5}$, and PM_1 was collected from January 2018 until March 2019 at the BCN (urban background) and MSY (regional background) twin supersites. To obtain the source apportionment of all PM sizes at both stations, a Positive Matrix Factorization model was used. The OP of the PM was determined by measuring levels of reactive oxygen species using dithiothreitol and ascorbic acid assays. These results will offer insights into the toxicity of different PM sources in BCN and MSY.

2. Methodology

2.1. Site descriptions

Samples of PM_{10}, $PM_{2.5}$, and PM_1 were collected from January 2018 until March 2019 at a set of twin stations in northeastern Spain, in the conurbation of Barcelona in conjunction with the regional background (Fig. 1). A summary of the station is presented in Table S2. The urban background air quality station is located in Barcelona, at IDAEA-CSIC (BCN; 41°23′14.5″N 2°06′55.6″E; 68 m a.s.l.) and close to Diagonal Avenue (Fig. 1, in black), which is one of the main traffic arteries of the city. Barcelona is located between the Mediterranean Sea to the east and the Collserola Chain of mountains to the west. With 1.7 million inhabitants (4.6 million in the metropolitan area), it is the second largest city in Spain and, based on population estimate, the fifth most populous urban area in the European Union (Demographia World Urban Areas, 2020). PM emissions from the city are mostly due to dense road traffic, industries, natural gas, and power plants used for energy production, the harbor, and the airport, making Barcelona one of the most PM-polluted areas in the Western Mediterranean (Amato et al., 2009a; Pandolfi et al., 2016; Querol et al., 2004a, 2004b, 2014). The mountain rural background station is located in the Montseny natural park (MSY; 41°46′45.63″N, 02°21′28.92″E; 720 m a.s.l.), which is in the Western Mediterranean Basin. The station is located 50 km to the north-northeast of Barcelona and 25 km from the Mediterranean coast. The MSY station is located far enough away from specific anthropogenic emission sources and has been shown to be representative of the regional background (Cusack et al., 2012; in 't Veld et al., 2021; Pandolfi et al., 2014, 2016; Pérez et al., 2008; Pey et al., 2009; Ripoll et al., 2015), although it can be impacted by emissions from urban and industrial areas under anticyclonic atmospheric conditions. The station is part of the European Aerosols, Clouds, and Trace Gases Research InfraStructure Network (ACTRIS) and the Global Atmosphere Watch (GAW).

2.2. PM sampling and chemical speciation

Roughly every four days between January 2018 until March 2019, 24 h PM_{10}, $PM_{2.5}$, and PM_1 filter samples were collected on the same day at each station (95 % of the samples were taken on the same day in BCN and MSY), with 71 % of the days having all 3 PM samples taken in BCN, and 73 % in MSY (any other days missed one or two sample sizes). This resulted in about a 100 samples per PM size per station (BCN: PM_{10} 94, $PM_{2.5}$ 102, PM_1 93; MSY: PM_{10} 105, $PM_{2.5}$ 106, PM_1 89).

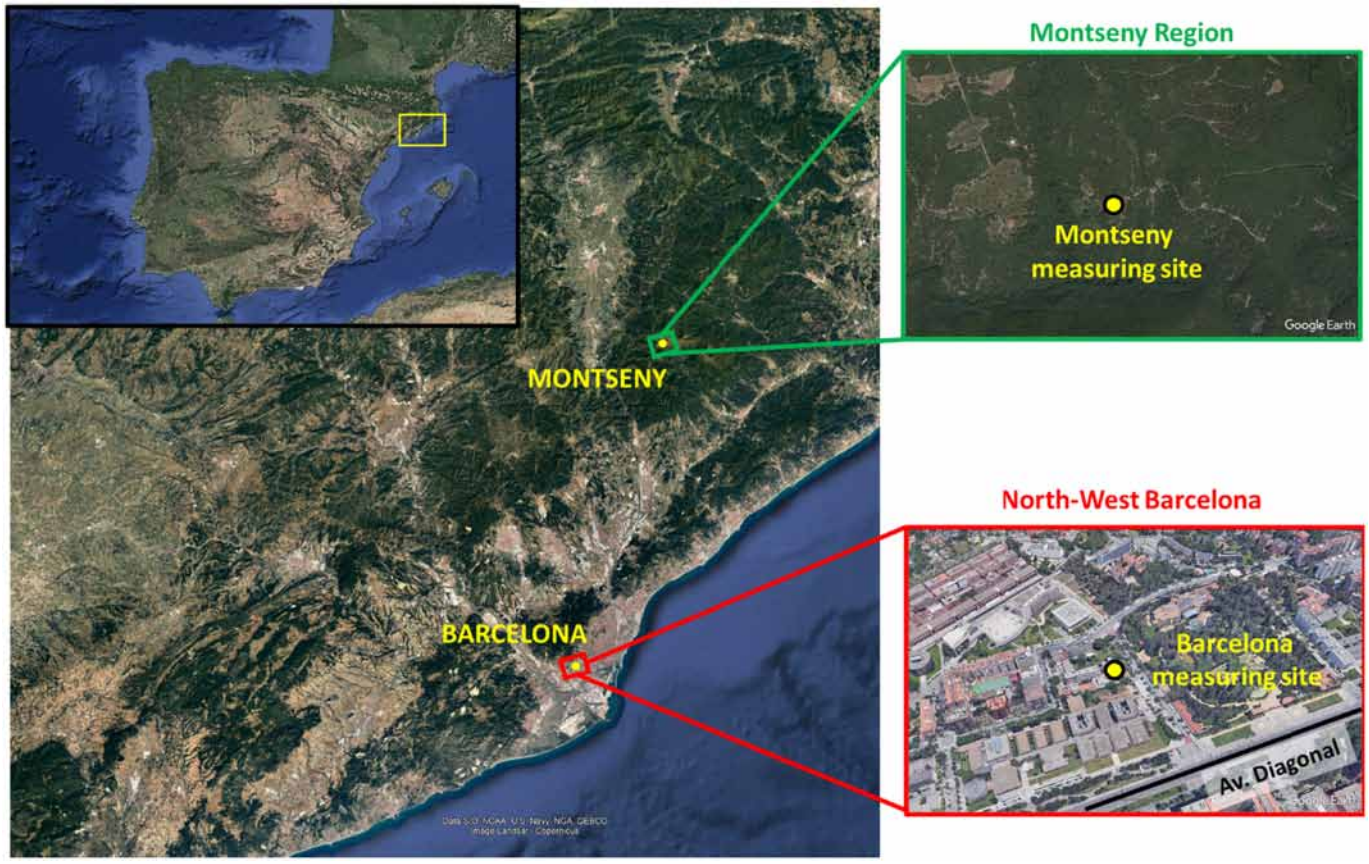

Fig. 1. Location of the Barcelona urban (BCN) station (41°23′14.5″N 2°06′55.6″E, 68 m a.s.l.) and the Montseny rural (MSY) station (41°46′45.63″N, 02°21′28.92″E, 720 m a.s.l.), both located in northeastern Spain, in the Catalonia region. Images were obtained from Google Earth.

The samples were collected using DH80 (DIGITEL, Switzerland/Austria) and CAVA/MSb (MCV, Spain) high volume samplers (30 m^3h^{-1}), equipped with PM_{10}, $PM_{2.5}$, and PM_1 inlets on 15-cm diameter ultrapure quartz microfiber filters (PALL). Every twelve filters samples of the same fitter box had a blank, which underwent the same sample treatment and measurements, and its values were subtracted from the corresponding samples. The averages concentrations of the blank are reported in Table S3. The PM mass on the filter were determined using the EN 12341 (PM_{10}) and EN 14907 ($PM_{2.5}$) gravimetrical procedures. In short, gravimetric concentration of PM was obtained by weighing the filter samples before and after sampling, after 48 h stabilization at 20 °C and 50 % RH (Alastuey et al., 2011). For PM_1 a similar method was used to the above reference method but with a 2 stages PM_1 inlet. After gravimetric analysis, samples were cut into quarters, with each undergoing a different treatment procedure. From one quarter, an area of 1.5 cm^2 was punched to measure the concentrations of organic carbon (OC) and elemental carbon (EC) via thermal-optical carbon analyzer (SUNSET), using the EUSAAR2 protocol (Cavalli and Putaud, 2010). To ensure the quality of the OC/EC method, a sucrose standard is used to see if the standard gives values are within an acceptable range.

The second quarter underwent acid digestion pretreatment (HNO_3:HF:$HClO_4$), and the resulting acidic solutions were subsequently analyzed using Inductively Coupled Plasma Atomic Emission Spectrometry (ICP-AES, ICAP 6500 Radial View, Thermo Fisher Scientific, US) to determine the concentration of major elements (Al, Ca, Cu, Fe, K, Mg, Mn, Na, P, and S) and Inductively Coupled Plasma Mass Spectrometry (ICP-MS, iCAP-RQ, Thermo fisher Scientific, US) to measure the concentration of trace elements (Li, Be, Sc, Ti, V, Cr, Mn, Co, Ni, Cu, Zn, Ga, Ge, As, Se, Rb, Sr, Y, Zr, Nb, Mo, Cd, Sn, Sb, Cs, Ba, La, Ce, Pr, Nd, Sm, Eu, Gd, Tv, Dy, Ho, Er, Tm, Yb, Lu, Hf, Ta, W, TI, Pb, Bi, Th, and U; Querol et al., 2001). The accuracy of the ICP-AES and ICP-MS analyses was investigated by analyzing 3–10 mg of the National Institute for Standards and Technology-1633b (fly ash) reference material loaded on a 150-mm blank filter (Amato et al., 2009a; Escrig Vidal et al., 2009).

The third quarter was leached in MilliQ water to determine the concentrations of NO_3^-, SO_4^{2-}, and Cl^- using ionic chromatography (IC, Dionex Aquion, Thermo Fisher Scientific). The Cl^- concentrations were previously identified as unreliable and were therefore removed from the source apportionment (in 't Veld et al., 2021). The accuracy of the IC was assured by performing a quality control protocol each batch, with each batch containing a months' worth of samples. This protocol consists out of three measurements. First an instrumental blank, to indicate any possible contamination of the equipment. Second, a standard of known concentration to observe if the retention times are still correct, and the accuracy and correlation of the calibration line. And finally, the injection of a quality control sample, which is a standard of known concentration but different than previous one.

Finally, NH_4^+ was determined using a specific electrode (ORION 9512HPBNWP ammonium selective electrode, Thermo Fisher Scientific) and potentiometer (ORION 4Star potentiometer, Thermo Fisher Scientific). The uncertainties and detection limits of the different species were calculated as described by Amato et al. (2009a, 2009b) and Escrig Vidal et al. (2009). In short, the detection limit was calculated according to the following equation:

$$LoD_j = 3 * \frac{\sqrt{\sigma_a^2 + \sigma_{BLK}^2}}{V_j} \quad (1)$$

where the limit of detection of species j is calculated using the uncertainty associated with the analytical procedure, σ_a, with the uncertainty of the blank samples, σ_{BLK}, and the volume of air sampled, V_j. σ_a^2 was calculated to be 0.01 for the ICP-AES, IC, and the thermal-optical carbon analyzer. For the ICP-MS this was set at 1.44e^{-5} for the relevant species.

The remaining quarter (or half a quarter in some cases) was used to determine the OP (see Section 2.3). This analysis was carried out at the Université Grenoble Alpes (UGA). Lastly, to estimate the SOA concentrations, the EC tracer method was applied, which has been used in previous studies (Castro et al., 1999; Dinoi et al., 2017; Wu and Yu, 2016; Yu et al., 2004). This method calculates the SOA according to the following equation:

$$SOA = (OC * n) - \left(\frac{OA}{EC * 1.1}\right)_{min} * (EC * 1.1) \quad (2)$$

To convert OC and EC values to OA, the OC values must be multiplied by *n*, a variable that depended on the location of the station. Values of 1.6 for BCN (Mohr et al., 2012) and 2.0 for MSY (Minguillón et al., 2011) were experimentally determined, and were close to the reference values of 1.7 for urban areas and 2.0 for rural areas (Turpin et al., 1997; Turpin and Huntzicker, 1995; Turpin and Lim, 2001). Meanwhile, EC must be multiplied by 1.1. The $(OC/EC)_{min}$ was determined by taking the second percentile of OC/EC ratios at BCN and MSY, which corresponded to 1.16 for BCN and 2.92 for MSY. Finally, K could also be used as a biomass burning tracer (K_{bb}) and was calculated as the difference between measured K and the sum of sea salt K (K_{ss}) and K in the crustal layer (K_{dust}; (Pachon et al., 2013; Reche et al., 2012; Yu et al., 2018). A detailed explanation of the calculations of K_{bb}, K_{dust}, and K_{ss} is given by in 't Veld et al. (2021), but can be summarized by the following equation:

$$K_{bb} = K_{total} - K_{ss} - K_{dust} \quad (3)$$

2.3. OP measurements

To determine the connection between chemical speciation and oxidative stress, an OP test was performed on each sample. The OP measures the intrinsic capacity of PM to generate reactive oxygen species that can oxidize the lungs. This is a good indicator of the toxic potential of chemical speciation, as various studies have linked respiratory diseases to reactive oxygen species, making it possible to gain insight into how PM affects human (Boukhenouna et al., 2018; Gangwar et al., 2020; Li et al., 2008; Liu and Chen, 2017; Park et al., 2009; Rosanna and Salvatore, 2012). The OP analysis was performed at IGE at UGA, following the procedure described in detail by Calas et al. (2018) and Daellenbach et al. (2020). In short, a combination of two assays was used: the ascorbic acid (AA) and dithiothreitol (DTT) assays. The difference between these assays is that each has a different sensitivity to different compounds. AA is the main antioxidant of the lung and is believed to be more sensitive to specific transition metals, such as copper, through allowing the reduction of H_2O_2 in OH*. In contrast, DTT is a thiol that functions as a surrogate of an antioxidant, mimicking the production of superoxide anions, thereby providing a balanced answer between transition metals and organic species (Calas et al., 2018; Chalovich and Eisenberg, 2005; Janssen et al., 2014). For both assays, the sample was extracted with a final concentration of 25 μg ml^{-1}. This was achieved by extracting the samples using a Gamble and dipalmitoyl phosphatidylcholine solution, which was then vortexed at maximum speed for 2 h at 37 °C.

The OP^{AA} was determined by measuring AA depletion. This was achieved with a plate-reader (TECAN spectrophotometer Infinite® M 1000 pro) at 265 nm using Greiner UV-Star® 96-well plates. A mixture of 120 μL Milli-Q water and 80 μL of PM suspension was created and then spiked with 24 nmol of AA (100 μL of 0.24 mM AA solution in Milli-Q water). After 2 min, the absorbance was measured every 4 min for a period of 30 min. A solution of 80 μL of 24.7 μM 1,4 naphthoquinone was used as a positive control in duplicate. In this way, the rate loss of AA could be determined in nmol min^{-1}.

The OP^{DTT} was determined using a similar method on a TECAN M200 Pro. The same plate reader was used as in the AA assay at 412 nm, but with 96-well CELLSTAR® multiwall plates from Greiner Bio-One®. In triplicate, a mixture of 205 μL of phosphate buffer (pH = 7.4) and 40 μL of PM suspension was made and then spiked with 12.5 nmol of DTT (50 μL of 0.25 mM DTT solution in phosphate buffer). For the final step, 50 nmol 5,5′-dithiobis (2-nitrobenzoic acid) was added, initiating the depletion reaction. The amount of DTT was quantified immediately and after 15 and 30 min of exposure. The same positive control was used as in the AA assay, but only using 40 μL. Knowing the AA and DTT depletion rates and the PM mass concentration in the wells, the normalization per cubic meter could be calculated for each assay and will be denoted as OP_v^{AA} (nmolAA min^{-1} m^{-3}) and OP_v^{DTT} (nmolDTT min^{-1} m^{-3}), respectively.

2.4. Source apportionment

The sources of the different PM sizes at both stations were obtained using a Positive Matrix Factorization (PMF) model (Paatero and Tapper, 1994), which was applied using the EPA PMFv5.0 software (Norris et al., 2014) developed by the U.S. Environmental Protection Agency (US-EPA). PMF is a multivariate factor analysis tool that decomposes one matrix—in this case, PM chemical compositions on different days—into two matrices: factor contributions and factor profiles. It achieves this by solving main chemical mass balance equations between measured species concentration and the sum of source contributions for those species:

$$X_{ij} = \sum_{k=1}^{p} g_{ik} * f_{kj} + e_{ij} \quad (4)$$

Here, *X* is the data matrix with *i* number of samples and *j* number of chemical species, *p* is the number of sources, *f* is the species profile of each source with a mass contribution *g*, and e_{ij} is the residual for each sample. The uncertainties of the different species were calculated as described by Amato et al. (2009a, 2009b) and Escrig Vidal et al. (2009), where the uncertainties were calculated by the following equation:

$$\sigma_{ij}^2 = \sqrt{\frac{\sigma_a^2 + \sigma_{BLK}^2}{V_i^2} + (\beta x_{ij})^2} \quad (5)$$

where the uncertainty of species *j* on filter *i*, σ_{ij}, is determined using the uncertainty associated with the analytical procedure, σ_a, with the uncertainty of the blank samples, σ_{BLK}, and the volume of air sampled, V_i. β is a coefficient which might account for any other additional sources of uncertainty, estimated to be 0.15 and x_{ij} is the concentration of species *j* on sample *i*.

The analytical uncertainties and the standard deviations of the different species in the blank filters were considered in the uncertainty calculations. For select species to be included in the model, a signal to noise (S/N) ratio > 1.5 was defined as a criterion indicating a "strong species", whereas an S/N ratio between 1.5 and 0.5 indicated a "weak species". Weak species uncertainties were increased by a factor of three. All species with a $S/N < 0.5$ were excluded from the model. The species included in each PMF are listed in Table S4.

One of the major challenges faced was the limited sample size, as only data from 15 months were used, resulting in approximately 100 samples per PM size per station. This is considered enough to obtain the recommended minimum of 100 samples needed for a PMF solution (Belis et al., 2014; Chen et al., 2010; Reff et al., 2007; Scerri et al., 2019). Although we obtained a good solution for the PM_{10} PMF model, however, we did not obtain an adequate solution for $PM_{2.5}$ and especially PM_1, due to the lower concentrations causing a very low S/N ratio for many chemical species, a bad bootstrapping result, and high base model displacement error resulting in a bad PM attribution of most sources.

To improve the robustness of our PMF model, a multisite solution was used by aggregating the BCN and MSY data into a single dataset for each PM size. Previous research has shown the feasibility of applying a multisite PMF to PM_{10} and $PM_{2.5}$ in the same study area (in 't Veld et al., 2021; Pandolfi et al., 2020). Applying the multisite solution did not, however, result in an adequate solution. While we were able to identify all sources that had previously been identified in our study area, some factors showed

Table 1
Identified Positive Matrix Factorization (PMF) factors and species used to identify sources of particulate matter.

Factor name	Main tracers	Remarks
OC-rich	OC	Some K, Cd, P present, seasonality
Secondary SO_4^{2-}	SO_4^{2-}, NH_4^+	Some OC, Strong seasonality
Secondary NO_3^-	NO_3^-, NH_4^+	Strong seasonality
Mineral	Al, Ti, Ga, Rb, Sr, Li, La	Seasonality in Montseny
Combustion	EC	Some OC, Traffic in BCN and mixed combustion in MSY
Sea spray	Na, Mg	Some SO_4^{2-}, NO_3^-
Road dust	Fe, Cr, Cu, Sn	Non-exhaust vehicle emissions
Heavy oil	V, Ni	Some Co, originates from shipping
Industry	Mn, Zn, Cd, Pb	Some K, Ni

null contribution to PM mass, and showed a bad bootstrapping and high base error estimation. Thus, to improve the robustness of our PMF model even further, a multisize solution was used by aggregating the results of PM_{10}, $PM_{2.5}$, and PM_1 from both stations into a single dataset, which improved the PM source apportionment drastically. At the time of writing, few studies have employed PMF solutions where multiple PM sizes were combined, but successful source apportionments have been applied by combining PM_{10} and $PM_{2.5}$ datasets. Amato et al. (2009a, 2009b) previously successfully performed a multi particle size PMF at a single site in BCN and Scerri et al. (2019) investigated the plausibility of a PMF source apportionment in the south of Italy, showing the viability of a multisize PMF model. Indeed, Scerri et al. (2019) concluded that the aggregated dataset created a more stable solution and, with some constraints, resulted in a good solution if similar sources affected both PM sizes.

A considerable amount of previous research has been performed in the study area regarding sources of PM_{10}, $PM_{2.5}$, and PM_1 (Amato et al., 2009b, 2016; Brines et al., 2019; in 't Veld et al., 2021; Minguillón et al., 2011; Moreno et al., 2011; Pandolfi et al., 2016, 2020; Pérez et al., 2016; Querol et al., 2007; Reche et al., 2012; Viana et al., 2013). This extensive research, which has applied PMF for all PM sizes, has separately identified the same sources for all PM sizes. To test the similarity between the chemical profiles of the multisize–multisite solution and previous multisite solutions (in 't Veld et al., 2021; Pandolfi et al., 2020), the Pearson Distance (PD) and the Similarity Identity Distance (SID) were measured between the source profiles, following Weber et al. (2019). The PD between the contribution-to-species (in %) of chemical species in the same attributed source was equal to 1 – *r*, where *r* is the Pearson coefficient. The SID was calculated according to:

$$SID = \frac{\sqrt{2}}{m} \sum_{j=1}^{m} \frac{|x_j - y_j|}{x_j + y_j} \quad (6)$$

Here, *x* and *y* are the relative masses of the PM of the sources and *m* is the number of common species between *x* and *y*. Pernigotti and Belis (2018) considered PD < 0.4 and SID < 1 as acceptable criterion for profile similarity. The found sources were compared to a 15-month-long (January 2017 – March 2018) PM_{10} multisite solution and a 10-year-long $PM_{2.5}$ solution (2009–2018; in 't Veld et al., 2021), with both comparisons meeting the previously stated criteria (Table S5). It can therefore be considered that the inorganic chemical profiles of the source contributions are similar for PM_{10}, $PM_{2.5}$, and PM_1. It is important to note that not all sources affect all PM sizes equally, as is the case for the Mineral source, which mainly affected PM_{10} and had a very small contribution to PM_1.

The optimal number of sources was selected by inspecting Q values, residuals, G space plots, and the physical meaning of the factors using previous expertise on PMF results in BCN and MSY (Amato et al., 2009a, 2009b, 2016; Brines et al., 2019; in 't Veld et al., 2021; Minguillón et al., 2011; Moreno et al., 2011; Pandolfi et al., 2016, 2020; Pérez et al., 2016; Querol et al., 2007; Reche et al., 2012; Viana et al., 2013). To confirm the optimal factor profiles of the PMF model, the data were also bootstrapped. Each dataset was bootstrapped 100 times with a minimum correlation R-value of 0.6. Finally, the model error was estimated using the base model displacement method.

2.5. OP apportionment

To determine the intrinsic toxicity of each chemical species and source, a multilinear regression (MLR) model was applied, with the results from the two (AA and DTT) assays set as the dependent variables and the source contributions from the PMF set as the explanatory variables. The computing was conducted using the Python module statsmodels 0.13.1 (Seabold and Perktold, 2010). The MLR model was as follows:

$$OP_{obs} = \beta_0 + (G_i * \beta_i) + \varepsilon \quad (7)$$

where OP_{obs} is a vector of size of the observed OP (either OP_v^{AA} or OP_v^{DTT} in nmol min^{-1} m^{-3}); *G* is the matrix of the mass contribution of the PM sources in μg m^{-3}; β_i is the intrinsic OP of the source and β_0 is the intercept (also called the coefficients), both in nmol min^{-1} μg^{-1}; and ε is the residual term that accounts for the misfit between the observations and the model. Furthermore, to improve the modeling further, a weighted least-square regression (WLS) was used to consider the uncertainties of the OP measurements (Weber et al., 2021). The uncertainties of the β coefficients were estimated by bootstrapping the solution 1000 times and randomly selecting 70 % of the samples for each coefficient to account for possible remaining extreme events.

3. Results and discussion

3.1. PM_{10}, $PM_{2.5}$, and PM_1 source apportionment

Aggregating the datasets of all 3 PM sizes (PM_{10}, $PM_{2.5}$, and PM_1) for both the BCN and MSY stations resulted in nine common sources being identified, which were OC-rich, Secondary SO_4^{2-}, Secondary NO_3^-, Mineral, Combustion, Sea Spray, Road dust, Heavy Oil, Industry. Each source was previously reported in the study area (Amato et al., 2009a; in 't Veld et al., 2021; Pandolfi et al., 2011, 2020). A detailed description of each source is described in the Supplementary, with a summary of the nine identified sources provided in Table 1. Table 2 presents the PM mass and the relative contribution of each source to the PM mass, and the contribution

Table 2
Concentrations and relative contributions of each source for each size of particulate matter (PM) at each station.

Factor	Barcelona			Montseny		
	PM_{10} (μgm^{-3})	$PM_{2.5}$ (μgm^{-3})	PM_1 (μgm^{-3})	PM_{10} (μgm^{-3})	$PM_{2.5}$ (μgm^{-3})	PM_1 (μgm^{-3})
OC-rich	3.24 (20 %)	1.98 (21 %)	1.44 (20 %)	2.25 (30 %)	1.73 (30 %)	1.71 (37 %)
Sec. NO_3^-	2.11 (13 %)	1.61 (17 %)	0.97 (14 %)	0.92 (12 %)	0.76 (13 %)	0.59 (13 %)
Sec. SO_4^{2-}	1.64 (10 %)	2.42 (25 %)	2.37 (33 %)	1.20 (16 %)	2.10 (37 %)	2.06 (45 %)
Industry	0.06 (0 %)	0.06 (1 %)	0.06 (1 %)	0.03 (0 %)	0.03 (0 %)	0.02 (0 %)
Sea spray	2.67 (17 %)	0.63 (3 %)	0.25 (3 %)	1.17 (15 %)	0.31 (5 %)	−0.06 (−1 %)
Combustion	1.56 (10 %)	1.45 (15 %)	1.61 (23 %)	0.19 (3 %)	0.22 (4 %)	0.21 (5 %)
Mineral	2.79 (18 %)	0.85 (9 %)	0.07 (1 %)	1.74 (23 %)	0.45 (8 %)	0.02 (0 %)
Heavy oil	0.39 (2 %)	0.32 (3 %)	0.33 (5 %)	0.06 (1 %)	0.07 (1 %)	0.06 (1 %)
Road dust	1.41 (9 %)	0.33 (3 %)	0.06 (1 %)	0.07 (1 %)	0.02 (0 %)	0.01 (0 %)

of each element to all nine sources is presented in Fig. 2, with detailed source profiles presented in Fig. S1.

Overall, concentrations of the sources were higher in BCN, especially in the case of anthropogenic sources, such as Combustion, Road Dust, Industry, Heavy Oil, and Secondary NO_3^-, due to the proximity to the sources to the site. Some sources, such as OC-rich and Mineral, also showed higher concentrations in BCN because the contributions were dominated by anthropogenic sources. Sea Spray also showed an increase in BCN due to its proximity to the sea. Finally, Secondary SO_4^{2-} showed similar concentrations in both stations due to its regional origin.

When comparing PM sizes, no significant differences were observed among Combustion, Heavy Oil, and Industry. All the other sources, including OC-rich (only between PM_{10} and $PM_{2.5}$ + PM_1, which had similar concentrations), showed a decrease in concentrations and relative composition with decreasing PM size. The only exception to this was Secondary SO_4^{2-}, which showed lower concentrations for PM_{10} than for $PM_{2.5}$ and PM_1 at both stations, as a results of lower NH_4^+ levels in PM_{10} compared to the other size fractions. This underestimation is a known phenomenon in our study area due to reactions between NH_4NO_3 and NaCl. NaCl originates mainly from the sea in the $PM_{10-2.5}$ size fraction and reacts with NH_4NO_3 to form NH_4Cl. As NH_4Cl is semi-volatile, an underestimation of NH_4 in PM_{10} occurs, which resulted in the underestimation of the Secondary SO_4^{2-} source for PM_{10} in our study area (Amato et al., 2009a; Pandolfi et al., 2012; Querol et al., 2001).

3.2. OP results and seasonality

3.2.1. Barcelona

The timeseries of OP per μg of PM (OP_m) and OP per m^3 of air (OP_v) for both assays (Fig. 3 (left)), shows that neither OP_v timeseries showed a seasonal pattern over the study period, regardless of the PM size. The lack of a seasonal pattern agrees with studies at other urban coastal sites in the Mediterranean area, such as for PM_{10} in Nice and Port de Bouc, France (Calas et al., 2019), or for $PM_{2.5}$ samples in Dunkerque, France (Moufarrej et al., 2020). The OP_m^{DTT} timeseries did not show a seasonal pattern either, which implies that the OP of the sources is stable throughout the year. In contrast, the OP_m^{AA} timeseries showed a slight seasonal pattern, with higher values in winter. The seasonal pattern for OP^{AA} is due to the metal sensitive nature of OP^{AA}, which favors anthropogenic sources which in general, have higher levels during the winter. Comparing the OP_m and OP_v levels among the 3 PM sizes showed higher levels for PM_{10} in comparison to $PM_{2.5}$ and PM_1. This indicates that a main driver of OP in BCN is within the 10–2.5 μm size range. Furthermore, the OP of $PM_{2.5}$ and PM_1 were in the same range. The lack of a difference means that another main driver of the OP levels measured in PM_1 must originate from the <1 μm size range, while a driver within the 2.5–1 μm size range is absent.

Currently, there is no standardized OP test procedure, which can hinder comparison with other studies due to the different methodologies used (Calas et al., 2018, 2019; Yang et al., 2014). Thus, in this work, we only compared our OP values with those of 18 stations (13 in France, five in Switzerland) from two studies with OP measurements also performed at the UGA to overcome differences due to methodological approaches (Grange et al., 2022; Weber et al., 2021). Each station's annual average OP_V^{DTT} and OP_V^{AA} values for PM_{10} and $PM_{2.5}$, when applicable, are summarized in Table 3. The OP_v levels in BCN are in the same range as most French stations in the case of OP_v^{DTT}, and most French and Swiss stations in the case of OP_v^{AA}. However, it must be noted that most French stations were sampled in 2013–2014 and that when comparing results obtained in Grenoble in 2013 with those obtained in 2017, a significant reduction was observed in OP_V^{DTT}, from 2.7 to 1.7 nmol min^{-1} m^{-3} (Weber et al., 2021). This decrease was

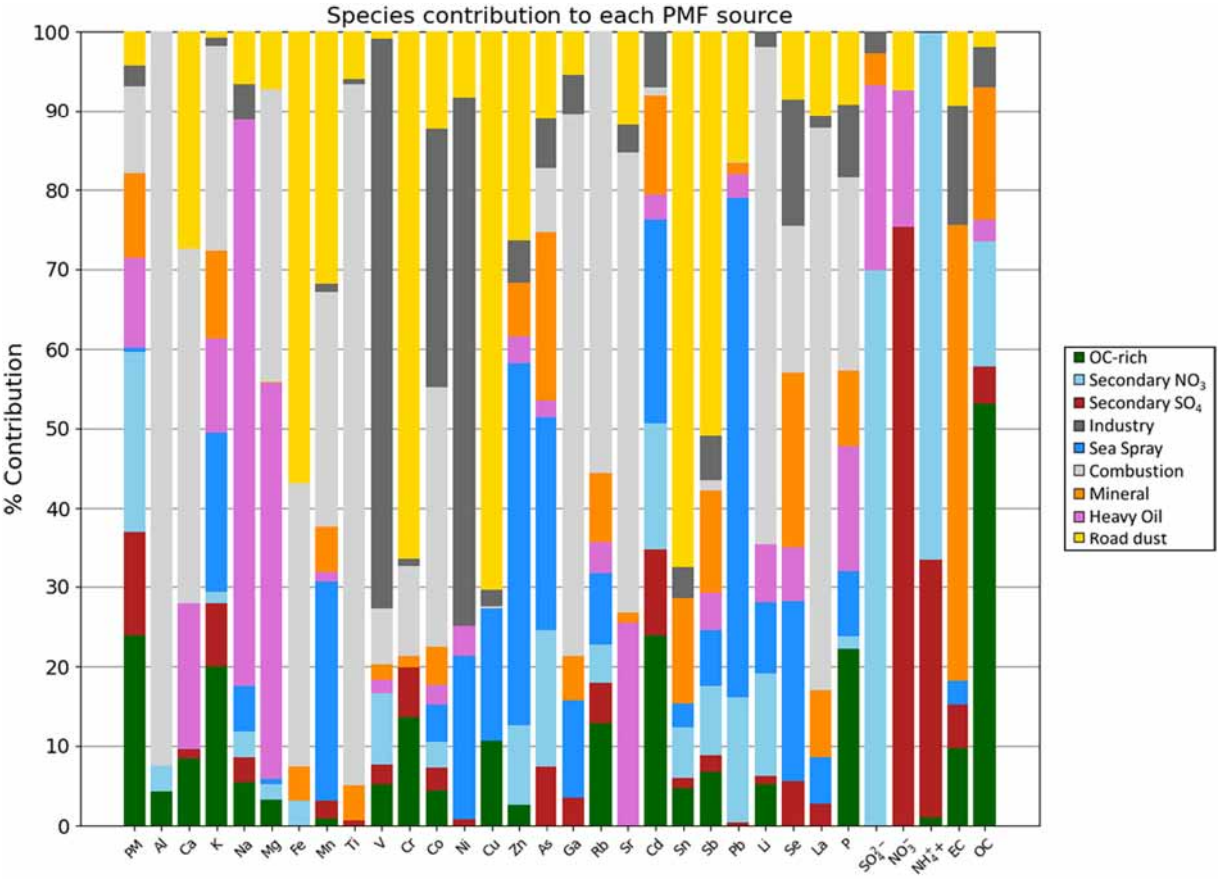

Fig. 2. Chemical speciation and source contribution to total mass of particulate matter (PM), according to the multisite multisize Positive Matrix Factorization (PMF) solution.

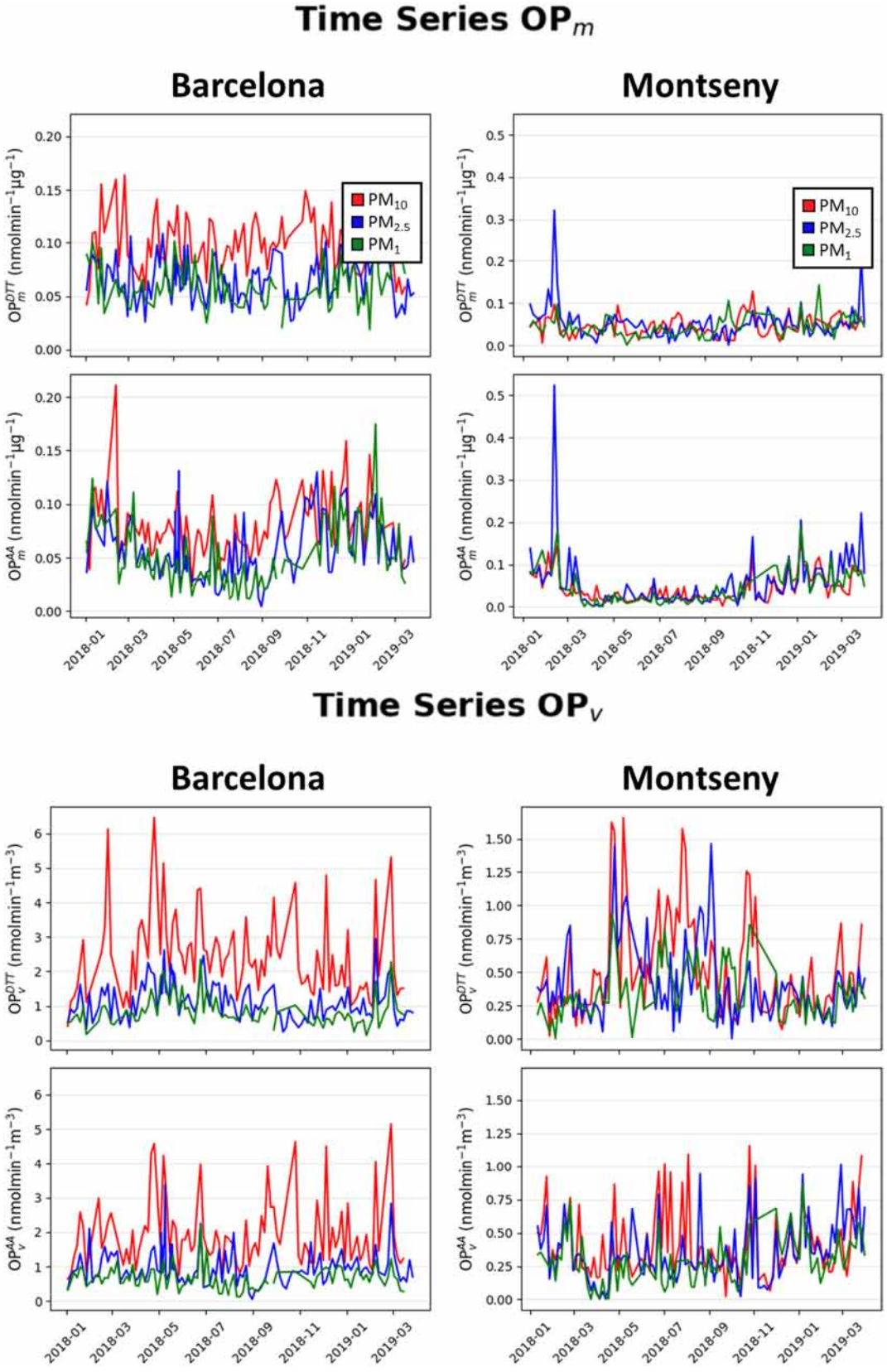

Fig. 3. Top: Timeseries of the intrinsic oxidative potential (OP) in Barcelona (BCN, left) and Montseny (MSY, right), for the OP^{DTT} and OP^{AA} in particulate matter (PM) size fractions PM_{10}, $PM_{2.5}$, and PM_1. Bottom: Timeseries of the OP_v in BCN (left) and MSY (right), for the OP^{DTT} and OP^{AA} in PM_{10}, $PM_{2.5}$, and PM_1.

primarily attributed to a decrease in PM_{10} in the study area (Borlaza et al., 2021a). Comparing the results in BCN with those in Grenoble and at Vif urban background sites (2017–2018), shows that the levels in BCN are significantly higher compared to those in France and Switzerland. The levels of OP_v^{AA} were much higher in BCN (1.9 nmol min^{-1} m^{-1} for PM_{10}) than in Nice or Marseille (1.0 and 0.5 nmol min^{-1} m^{-3}, respectively), which are

Table 3
Top: Information regarding each measurement site, country of origin, station type, sample period, and study reference. (ES = Spain, FR = France, CH = Switzerland). Bottom, Left: Sorted values of the OP_V^{DTT} for particulate matter (PM) fractions PM_{10} and $PM_{2.5}$; Right: Sorted values of the OP_V^{AA} for PM_{10} and $PM_{2.5}$. Stations from this study are in Italics.

Site	Country	Type	Year	Reference
Barcelona	*ES*	*Urban Background*	*Jan 2018 – Mar 2019*	*This study*
Montseny	*ES*	*Rural Background*	*Jan 2018 – Mar 2019*	*This study*
Passy	FR	Urban Valley	Nov 2013 – Oct 2014	(Weber et al., 2021)
Grenoble	FR	Urban Background	Mar 2017 – Mar 2018	(Weber et al., 2021)
Nogent	FR	Urban Background	Jan 2013 – May 2014	(Weber et al., 2021)
Roubaix	FR	Traffic	Jan 2013 – May 2014	(Weber et al., 2021)
Marseille	FR	Urban Background	Jan 2015 – Dec 2015	(Weber et al., 2021)
Strasbourg	FR	Traffic	April 2013 – April 2014	(Weber et al., 2021)
Chamoix	FR	Urban valley	Nov 2013 – Nov 2014	(Weber et al., 2021)
Nice	FR	Urban traffic	Jul 2014 – May 2015	(Weber et al., 2021)
Aix-en-provence	FR	Urban background	Aug 2013 – Jul 2014	(Weber et al., 2021)
Talence	FR	Urban background	Mar 2012 – Mar 2013	(Weber et al., 2021)
Marnaz	FR	Urban valley	Nov 2013 – Oct 2014	(Weber et al., 2021)
Port-de-bouc	FR	Industrial	Jun 2014 – May 2015	(Weber et al., 2021)
Vif	FR	Urban background	Mar 2017 – Mar 2018	(Weber et al., 2021)
Bern	CH	Urban-Traffic	June 2018 – May 2019	(Grange et al., 2022)
Zürich	CH	Urban	June 2018 – May 2019	(Grange et al., 2022)
Cadenazzo	CH	Rural	June 2018 – May 2019	(Grange et al., 2022)
Payerne	CH	Rural	June 2018 – May 2019	(Grange et al., 2022)
Basel	CH	Suburban	June 2018 – May 2019	(Grange et al., 2022)

		OP_V^{DTT}				OP_V^{AA}	
Site	Country	PM_{10}	$PM_{2.5}$	Site	Country	PM_{10}	$PM_{2.5}$
Passy	FR	4.4	–	Bern	CH	4.1	1.6
Bern	CH	2.9	1.1	Chamoix	FR	2.6	–
Nogent	FR	2.7	–	Passy	FR	2.2	–
Roubaix	FR	2.6	–	Nogent	FR	2.2	–
Marseille	FR	2.6	–	Roubaix	FR	2.1	–
Barcelona	*ES*	*2.5*	*1.2*	*Barcelona*	*ES*	*1.9*	*1.0*
Strasbourg	FR	2.4	–	Aix-en-provence	FR	1.7	–
Chamoix	FR	2.3	–	Zürich	CH	1.7	0.8
Nice	FR	2.2	–	Cadenazzo	CH	1.7	1.2
Aix-en-provence	FR	1.9	–	Marnaz	FR	1.6	–
Talence	FR	1.8	–	Grenoble	FR	1.5	–
Marnaz	FR	1.8	–	Vif	FR	1.5	–
Port-de-bouc	FR	1.8	–	Strasbourg	FR	1.3	–
Grenoble	FR	1.5	–	Basel	CH	1.2	0.7
Vif	FR	1.3	–	Nice	FR	1.0	–
Zürich	CH	1.3	0.8	Talence	FR	1.0	–
Cadenazzo	CH	1.0	0.7	Payerne	FR	0.7	0.4
Payerne	CH	0.8	0.6	Port-de-bouc	FR	0.6	–
Basel	CH	0.8	0.6	Marseille	FR	0.5	–
Montseny	*ES*	*0.5*	*0.4*	*Montseny*	*CH*	*0.4*	*0.3*

also Mediterranean coastal cities. This increase in Barcelona must therefore come from additional anthropogenic sources around the city, most likely from traffic, metal and cement industry, or shipping, as these are the major sources of OP_v^{AA} (see Section 3.3.1).

3.2.2. Montseny

Very low OP_v values were obtained for both assays with MSY samples ($OP_v^{AA} < 1$ nmol min^{-1} m^{-3} and $OP_v^{DTT} < 1.5$ nmol min^{-1} m^{-3}) regardless of PM size, which is a typical pattern for a rural site (Fig. 3, right). Compared to stations in France and Switzerland, the OP values were lowest both for OP_v^{DTT} and for OP_v^{AA}, and for PM_{10} and $PM_{2.5}$, due to the rural typology of MSY. The lower levels compared to the other rural stations (Cadenazzo and Payerne, Switzerland) is likely due to the fact that the Swiss stations were more affected by biomass burning, with a known higher intrinsic OP compared to our OC-rich source measured in MSY (Section 3.3.2.). Neither assay showed a clear seasonal pattern, however, which was also observed for the OP_m obtained from both assays. In contrast to in BCN, the mean OP_m and OP_v levels of OP^{AA} and OP^{DTT} were in the same range for all PM sizes in MSY. The lack of a significant difference among the 3 PM sizes in MSY indicates that the main OP drivers originate from PM_1. At the time of writing, we are not aware of any articles that have been published regarding long-term OP measurements for PM_1.

Comparing the two stations, it is evident that for a given PM mass concentration, OP_v is higher in BCN than in MSY. This difference is the result of the local anthropogenic activities in BCN and the large distance to MSY. For all 3 PM sizes, BCN observations displayed a higher capacity to induce oxidative stress than did those from MSY, with PM_{10} evidencing the most pronounced difference.

3.3. Linking OP with PM source contributions

To determine the main driver(s) of OP for each PM size, two methods were applied to explain the relationship between OP and PMF sources or chemical speciation. The first method was a Pearson correlation test between OP_v and the sources and chemical speciation. Secondly, an MLR analysis was applied to search for the major relationships between the PMF sources (in $\mu g m^{-3}$) and OP_v^{AA} and OP_v^{DTT}. Adding the MLR to the Pearson correlation coefficient is useful because the correlation on its own is limited for linking OP with sources and/or chemistry, as a good correlation does not always imply causality (Weber et al., 2021). For instance, as shown in Fig. 5, Secondary NO_3^- and Secondary SO_4^{2-}

were significantly correlated with OP_v, even though $(NH_4)_2SO_4$ and NH_4NO_3 have been shown to have a negligible OP (Daellenbach et al., 2020; Grange et al., 2022; Weber et al., 2021), but the respective sources may co-emit oxidizing components that were not measured in this study.

3.3.1. Barcelona

In BCN, the PM apportionment model indicated that >45 % of the PM_{10} (46 %), $PM_{2.5}$ (67 %), and PM_1 (80 %) mass load was attributed to OC-rich, Secondary SO_4^{2-}, and Combustion sources. It must be noted that in BCN, the OC-rich source is a combination of SOA and POA (see Supplementary Information). This was confirmed with by showing a significant difference between the correlation coefficients of OC and OP^{DTT} (r = PM_{10}: 0.70; $PM_{2.5}$: 0.56; PM_1: 0.49), and between OP^{DTT} and the estimated SOA (r = PM_{10}: 0.49; $PM_{2.5}$: 0.43; PM_1: 0.40), which were also observed between OP_v^{AA} and OC (r = PM_{10}: 0.74; $PM_{2.5}$: 0.57; PM_1: 0.33), and between OP_v^{AA} and SOA (r = PM_{10}: 0.45; $PM_{2.5}$: 0.41; PM_1: unsignificant). The only other significant mass contributors were the Mineral and Sea Spray sources in PM_{10}, as they have a major coarse size mode and, therefore, are two of the largest mass-contributing sources to PM_{10}.

3.3.1.1. PM_{10}. Overall, the main OP drivers originated from anthropogenic sources from the city. The intrinsic OP of PM_{10} was dominated by the Heavy Oil and Combustion sources, having a high intrinsic OP for the DTT assay, with 0.437 ± 0.005 and 0.242 ± 0.002 nmol min^{-1} μg^{-1}, respectively, and the OP^{AA} assay, with 0.485 ± 0.004 and 0.357 ± 0.001 nmol min^{-1} μg^{-1}, respectively (Table 4A and B; Figs. S3 and S4). The metal-sensitive AA assay indicated that Industry was the most dominant source, significantly higher than the other sources, with 1.480 ± 0.047 nmol min^{-1} μg^{-1}. The high intrinsic OP of combustion, road dust, and industry is most likely driven by the chemicals that compose the sources (Fig. 4) but might also be caused by the high content of Black Carbon (BC). Toxicological evidence has shown that BC itself is poorly reactive alone but can function as a Trojan horse and carry metals, or quinones that substantially contribute to OP (Chu et al., 2017; Li et al., 2013; Niranjan and Thakur, 2017). The daily averaged OP exposure showed the same sources as the main drivers of the intrinsic OP. The OP_v^{DTT} and OP_v^{AA} were mostly driven by the Heavy Oil and Combustion sources, with 0.200 and 0.363 nmol min^{-1} m^{-3}, respectively for the OP_v^{DTT} assay and 0.222 and 0.534 nmol min^{-1} m^{-3} for the OP_v^{AA} assay. The OC-rich source also showed a strong influence, being the primary driver in the OP_v^{DTT} assay, with 0.473 nmol min^{-1} m^{-3}, and ranked third in the OP_v^{AA} assay, with 0.220 nmol min^{-1} m^{-3}. This shows that there is not a single source responsible for the high OP_v in BCN.

Comparing this observation with observation in France, similar drivers of OP were found for PM_{10}. (Weber et al., 2021) reported that road traffic was the most prominent source driving OP_v^{DTT}, which was traced by OC, EC, Cu, Fe, Sn, and Sb. In our study, these tracers were spread among three different sources: OC-rich (OC), Combustion (EC), and Road Dust (Cu, Fe, Sn, and Sb). (Grange et al., 2022) also reported that in Switzerland, PM_{10} and $PM_{2.5}$ OP_v^{DTT} were driven by two major anthropogenic sources, road traffic and wood combustion, which have similar tracers to those previously discussed. Our observations are therefore in line with what has been observed in France and Switzerland, with OC-rich and Combustion sources driving the OP_v^{DTT}. More concretely, OC and EC concentrations appear to be the leading factor controlling OP_v^{DTT}, due to the higher daily averaged OP exposure and higher Pearson correlation (OC: 0.70; EC: 0.68; Cu: 0,54; Fe: 0.63; Sb: 0.55; Sn: 0.55; Fig. 4). In both France and Switzerland, the OP_v^{AA} was driven by road traffic and biomass burning, which was traced by OC, EC, and K^+. The same was observed in our study, with Combustion and OC-rich being the first- and third-ranked sources, respectively. In our study, however, the biomass burning source could not be separately identified due to its expected very low contribution to PM, making any direct comparison difficult. It is worth pointing out that an important finding of this study, also evidenced in (Weber et al., 2021) and (Grange et al., 2022), is the lack of a clear relationship between mass contribution and intrinsic OP, which shows the importance of focusing research on health-related properties rather than on the mass of each emission source.

One significant difference observed in our results when compared to those obtained at monitoring stations in France and Switzerland was the influence of Heavy Oil, which was not identified in France or Switzerland due to the distance from shipping emissions for most sites under study. Perrone

Table 4
(A) The intrinsic OP^{DTT} of all sources for particulate matter (PM) fractions PM_{10}, $PM_{2.5}$, and PM_1 at both stations. Units expressed in nmol min^{-1} μg^{-1}. (B) The intrinsic OP^{AA} of all sources for particulate matter (PM) fractions PM_{10}, $PM_{2.5}$, and PM_1 at both stations. Units expressed in nmol min^{-1} μg^{-1}.

A

	Barcelona						Montseny					
Factor	PM_{10}		$PM_{2.5}$		PM_1		PM_{10}		$PM_{2.5}$		PM_1	
OC-rich	0.169	± 0.001	0.041	± 0.001	0.044	± 0.001	0.026	± 0.001	0.031	± 0.001	0.042	± 0.000
Sec. NO_3	−0.016	± 0.001	0.015	± 0.001	−0.043	± 0.001	−0.033	± 0.001	0.007	± 0.001	−0.016	± 0.001
Sec. SO_4	0.120	± 0.001	0.075	± 0.001	0.036	± 0.001	0.049	± 0.001	0.041	± 0.001	0.015	± 0.000
Industry	−0.153	± 0.038	−0.066	± 0.032	4.652	± 0.069	−0.075	± 0.033	−1.565	± 0.036	0.905	± 0.022
Sea Spray	0.076	± 0.001	0.161	± 0.004	−0.394	± 0.014	0.031	± 0.001	−0.146	± 0.005	0.232	± 0.006
Combustion	0.242	± 0.002	0.072	± 0.002	0.046	± 0.001	−0.295	± 0.004	0.216	± 0.004	−0.073	± 0.002
Mineral	0.080	± 0.001	0.000	± 0.002	0.011	± 0.010	0.044	± 0.000	0.017	± 0.002	0.282	± 0.002
Heavy Oil	0.437	± 0.005	0.158	± 0.004	0.243	± 0.003	−0.281	± 0.009	0.223	± 0.013	0.512	± 0.006
Road dust	0.188	± 0.005	1.397	± 0.020	0.487	± 0.026	2.585	± 0.016	1.877	± 0.030	2.864	± 0.018

B

	Barcelona						Montseny					
Factor	PM_{10}		$PM_{2.5}$		PM_1		PM_{10}		$PM_{2.5}$		PM_1	
OC-rich	0.078	± 0.001	0.011	± 0.001	0.041	± 0.001	0.084	± 0.001	0.036	± 0.000	0.002	± 0.000
Sec. NO_3	0.022	± 0.001	0.042	± 0.000	−0.028	± 0.001	0.047	± 0.001	−0.003	± 0.001	−0.015	± 0.001
Sec. SO_4	0.019	± 0.001	0.027	± 0.001	0.004	± 0.001	−0.079	± 0.001	−0.047	± 0.001	−0.028	± 0.000
Industry	1.480	± 0.047	1.760	± 0.022	4.362	± 0.034	2.836	± 0.033	5.085	± 0.028	3.982	± 0.022
Sea Spray	0.046	± 0.002	−0.008	± 0.002	0.199	± 0.007	0.015	± 0.001	−0.047	± 0.003	0.231	± 0.007
Combustion	0.357	± 0.001	0.102	± 0.001	0.029	± 0.001	−0.361	± 0.004	−0.248	± 0.005	0.000	± 0.003
Mineral	0.056	± 0.001	0.039	± 0.001	−0.243	± 0.005	−0.014	± 0.000	0.062	± 0.001	−0.095	± 0.002
Heavy Oil	0.485	± 0.004	−0.111	± 0.002	−0.071	± 0.002	−0.100	± 0.009	−0.023	± 0.007	−0.060	± 0.005
Road dust	0.020	± 0.003	0.709	± 0.009	0.342	± 0.013	1.131	± 0.016	0.791	± 0.030	0.665	± 0.018

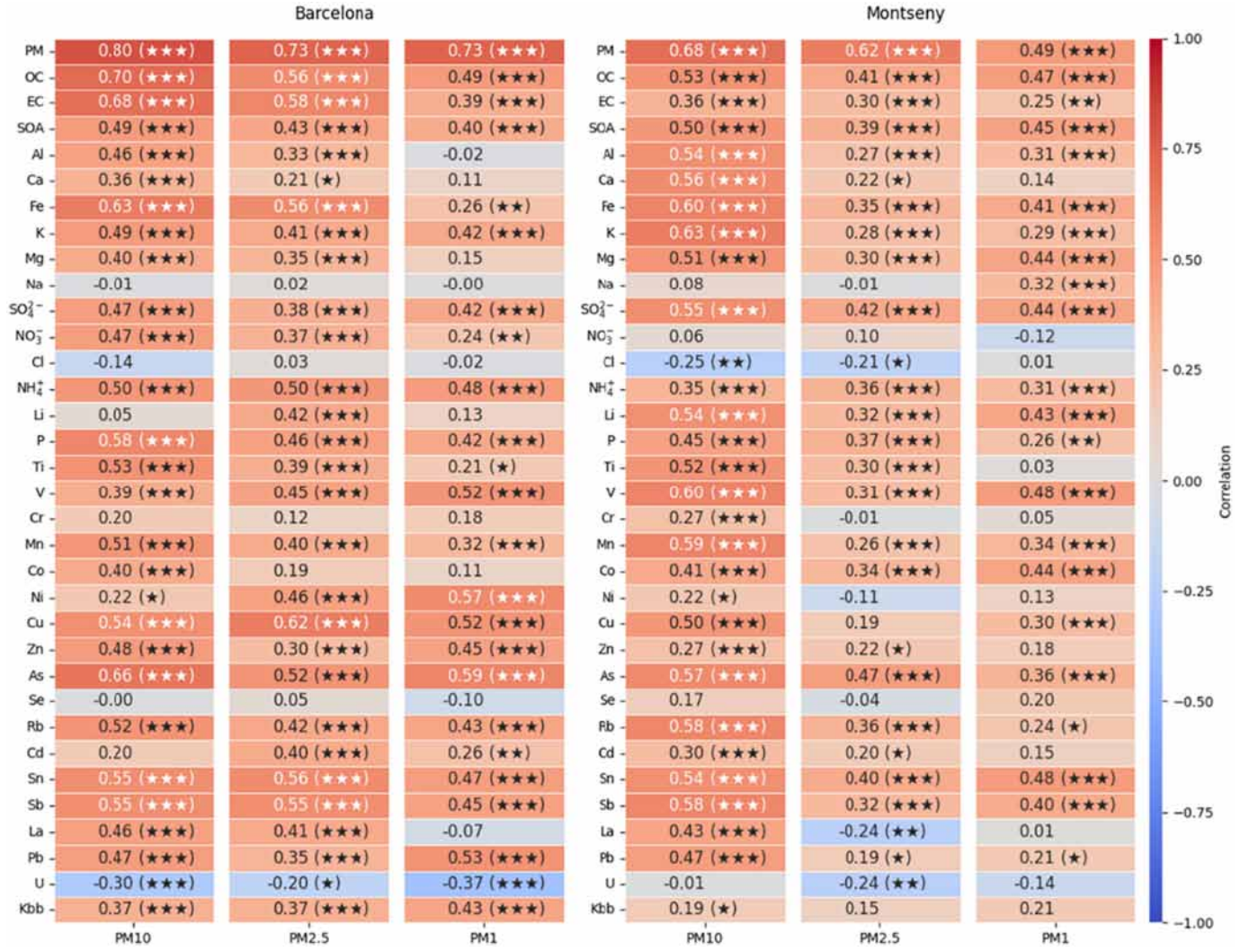

Fig. 4. Pearson's correlation coefficients between OP_v^{DTT} and the chemical species for each size of particulate matter (PM) at each site, with statistical significance represented by *** for $p < 0.001$, ** for $p < 0.01$, and * for $p < 0.05$.

et al. (2019) reported that Heavy Oil was the main factor governing OP_v^{AA} when studying OP in PM_{10} and $PM_{2.5}$ samples collected in a coast city in Italy, similar to what has previously been observed in BCN (Contini et al., 2011; Moldanová et al., 2009; Perrone et al., 2019; Viana et al., 2014). In our study, Heavy Oil had a significant contribution to OP_v^{DTT}, regardless of the PM size fraction, and also OP_v^{AA} in PM_{10}.

It is worth noting that the Pearson correlation analysis also showed Combustion and Road Dust as important drivers of OP_v^{DTT} in PM_{10} but, surprisingly, showed a very low correlation with the OC-rich source, even though the correlation between OC and OP_v^{DTT} was high (Figs. 4 and 6). This again highlights the fact that, although the Pearson correlation is a good indicator of the importance of certain sources, it should preferably be used in combination with a MLR model.

3.3.1.2. $PM_{2.5}$. The intrinsic OP^{DTT} assay in $PM_{2.5}$ was dominated by Road Dust, with 1.397 ± 0.020 nmol min^{-1} μg^{-1}. This significant role in the intrinsic OP of $PM_{2.5}$ is attributed to the fact that specific metals from vehicle wear fall mostly in the $PM_{2.5}$ fraction (Mohammed et al., 2017; Moreno et al., 2006; Wang et al., 2006). Meanwhile, the intrinsic OP^{AA} assay was still dominated by Industry, with 1.760 ± 0.022 nmol min^{-1} μg^{-1}, followed by Road Dust, with 0.709 ± 0.009 nmol min^{-1} μg^{-1} (Table 5A; Fig. S4). The contribution of Road Dust in BCN mostly comes from non-exhaust traffic emissions (Amato et al., 2016). In BCN, Road Dust showed a high correlation with OP^{DTT} in PM_{10} ($r = 0.65$) and $PM_{2.5}$ ($r = 0.61$), but a low one in PM_1 ($r = 0.24$). The same pattern was observed in the case of the OP^{AA} assay ($r = 0.75$ in PM_{10}, r = 0.65 in $PM_{2.5}$, and $r = 0.32$ in PM_1). This resulted in Road Dust being the main driver of the daily averaged OP exposure in OP_v^{DTT}, with 0.341 nmol min^{-1} m^{-3}, and in OP_v^{AA}, with 0.173 nmol min^{-1} m^{-3}. Combustion was the second most important driver, with 0.141 nmol min^{-1} m^{-3}, showing the impact of traffic on this PM size (Figs. 4, 5, S3, and S4; Table 5A and B).

3.3.1.3. PM_1. Finally, PM_1 was dominated by Industry in both the intrinsic OP^{DTT}, with 4.652 ± 0.069 nmol min^{-1} μg^{-1}, and the intrinsic OP^{AA}, with 4.362 ± 0.034 nmol min^{-1} μg^{-1}, far above any of the other sources. The Industry source represents a mixture of common tracers in BCN from industrial activities such as smelters and cement kilns (Amato et al., 2009a; Cusack et al., 2012; in 't Veld et al., 2021; Pandolfi et al., 2016; Pérez et al., 2016; Querol et al., 2007, 2014). The size distribution of the industrial PM contribution fell mainly in PM_1, due to the high temperatures involved during industrial processes, which would explain this high intrinsic OP. This also resulted in Industry being the main driver of OP_v^{DTT} and OP_v^{AA}, with 0.228 and 0.214 nmol min^{-1} m^{-3}, respectively, which are values much higher than those obtained for PM_{10} and $PM_{2.5}$ (Table 4A and 5A; Figs. S3

Table 5
(A) The daily median averaged human exposure to OP^{DTT} from all sources of particulate matter (PM) fractions PM_{10}, $PM_{2.5}$, and PM_1 at both stations. Units expressed in nmol min^{-1} m^{-3}. (B) The daily median averaged human exposure to OP^{AA} from all sources of particulate matter (PM) fractions PM_{10}, $PM_{2.5}$, and PM_1 at both stations. Units expressed in nmol min^{-1} m^{-3}.

A

	Barcelona			Montseny		
Factor	PM_{10}	$PM_{2.5}$	PM_1	PM_{10}	$PM_{2.5}$	PM_1
OC-rich	0.473	0.066	0.063	0.049	0.044	0.065
Sec. NO_3	−0.016	0.011	−0.021	−0.019	0.002	−0.005
Sec. SO_4	0.106	0.132	0.067	0.043	0.059	0.023
Industry	−0.007	−0.003	0.228	−0.002	−0.030	0.015
Sea Spray	0.104	0.053	−0.009	0.020	−0.019	−0.012
Combustion	0.363	0.100	0.057	−0.061	0.055	−0.016
Mineral	0.188	0.000	0.001	0.047	0.048	−0.008
Heavy Oil	0.200	0.060	0.103	−0.017	0.015	0.022
Road dust	0.172	0.341	0.016	0.121	0.032	0.031

B

	Barcelona			Montseny		
Factor	PM_{10}	$PM_{2.5}$	PM_1	PM_{10}	$PM_{2.5}$	PM_1
OC-rich	0.220	0.018	0.060	0.157	0.050	0.004
Sec. NO_3	0.022	0.029	−0.013	0.0.028	−0.001	−0.005
Sec. SO_4	0.017	0.047	0.008	−0.070	−0.069	−0.043
Industry	0.070	0.085	0.214	0.065	0.098	0.068
Sea Spray	0.062	−0.003	0.004	0.009	−0.006	−0.012
Combustion	0.534	0.141	0.036	−0.074	−0.055	0.000
Mineral	0.131	0.027	−0.024	−0.015	0.020	0.003
Heavy Oil	0.222	−0.042	−0.030	−0.006	−0.002	−0.003
Road dust	0.018	0.173	0.011	0.053	0.013	0.007

and S4). This suggests the potential impact of Industry on health, which was not observed for PM_{10} and $PM_{2.5}$.

3.3.2. Montseny

As expected, PM source masses were significantly lower in MSY than in BCN due to the distance of the site from most sources. Like BCN, the OC-rich and Secondary SO_4^{2-} sources accounted for >50 % of the PM mass in PM_{10} (54 %), $PM_{2.5}$ (76 %), and PM_1 (87 %), with only Mineral and Sea Spray also being significant contributors to PM_{10} (Table 2). The biggest difference from BCN was the low mass contribution of Combustion. The OC-rich source mostly consisted of biogenic SOA in MSY, which was confirmed by the chemical speciation showing a similar correlation between OP_v^{DTT} and OC (r = PM_{10}: 0.53; $PM_{2.5}$: 0.41; PM_1: 0.47) and estimated SOA (r = PM_{10}: 0.50; $PM_{2.5}$: 0.39; PM_1: 0.45), and between OP_v^{AA} and OC (r = PM_{10}: 0.34; $PM_{2.5}$: 0.20) and estimated SOA (r = PM_{10}: 0.29).

In MSY, the intrinsic OP^{DTT} was dominated by Road Dust for all PM sizes, with values of 2.585 ± 0.016, 1.877 ± 0.030, and 2.864 ± 0.018 nmol min^{-1} μg^{-1} for PM_{10}, $PM_{2.5}$, and PM_1, respectively (Table 4B; Fig. S5). Meanwhile, the intrinsic OP^{AA} assay was dominated by Industry, with 2.836 ± 0.033, 5.085 ± 0.028, 3.982 ± 0.022 nmol min^{-1} μg^{-1} for PM_{10}, $PM_{2.5}$, and PM_1, respectively. All other sources were significantly lower, although Road Dust also significantly contributed to the intrinsic OP^{AA} assay, with values of 1.131 ± 0.016, 0.791 ± 0.030, and 0.665 ± 0.018 nmol min^{-1} μg^{-1} for PM_{10}, $PM_{2.5}$, and PM_1, respectively (Figs. 4B and S6).

The significantly low mass contributions of Industry and Road Dust resulted in different sources driving the daily averaged OP exposure. In PM_{10}, Road Dust was the main driver of OP_v^{DTT}, with 0.121 nmol min^{-1} m^{-3}, which is much lower than the value associated with the main governing source in BCN (OC-rich = 0.473 nmol min^{-1} m^{-3}). Meanwhile, the OC-rich source was the main driver of OP_v^{AA}, with 0.157 nmol min^{-1} m^{-3}. $PM_{2.5}$ had no clear main drivers at MSY, with a similar dependency on multiple sources, such as Secondary SO_4^{2-}, Combustion, OC-rich, and Road Dust, all in the same range, between 0.032 and 0.059 nmol min^{-1} m^{-3}, which is over five times lower than levels in BCN. The OP_v^{AA} daily averaged OP exposure was mostly driven by Industry, with 0.098 nmol min^{-1} m^{-3}. Finally, PM_1 daily averaged OP exposure of OP_v^{DTT} was driven by the OC-rich source (0.065 nmol min^{-1} m^{-3}), whereas Industry drove the OP_v^{AA} (0.068 nmol min^{-1} m^{-3}). Values for both of these sources were three times lower than the highest-ranked source in BCN (Table 5A and B; Figs. S5 and S6).

Borlaza et al. (2021a) measured the OP of samples collected at a rural station for 3.5 years (2017–2020) in France and reported that mineral dust and sulfate-rich sources drove OP_v^{DTT}, while biomass burning drove OP_v^{AA}. These results are different than those obtained at MSY, likely due to the different source attributions. For example, elements attributed to the mineral dust source in the work of Borlaza et al. (2021b) were separated into Mineral and Road Dust in our study. Certain elements, however, like Fe, were found to drive the OP_v^{DTT} in both studies. Another example is Zn, which was attributed to the sulfate-rich source by (Borlaza et al., 2021b), whereas in our solution it was identified as a main tracer of Industry. In our study, the Pearson correlation with K_{bb} was moderate ($r = 0.42$), showing that biomass burning can be an important driver of OP_v^{AA} at this station; however, without a clear identification of a biomass burning source, the actual impact of the source on human health could not be accurately determined.

The extremely low OP_v values observed at the MSY station for all PM sizes, when compared to those obtained in BCN, emphasize that most of the OP_v in BCN comes from local sources, with regional sources playing a minor role.

4. Conclusions

To our knowledge, this is the first study successfully comparing oxidative potential (OP) levels and OP source apportionment of PM_1, $PM_{2.5}$, and PM_{10} simultaneously over a year-long study period. One known flaw of this study is that no ideal Positive Matrix Factorization solution was found if the intention was to compare the OP of the same source profiles for the urban (BCN) and regional (MSY) background sites. Additionally, there was a PM attribution underestimation for the source contribution of Secondary SO_4^{2-} to PM_{10} at both stations due to the underestimation of NH_4^+ in PM_{10} caused by reactions between NH_4NO_3 and NaCl in the $PM_{10-2.5}$ size fraction.

In BCN, the OP levels per m^3 (OP_v) of the DTT assay and AA assay were significantly higher for PM_{10} than for $PM_{2.5}$ and PM_1, which were both in the same range. This means that the main driver of OP in BCN is in the PM_{10} and PM_1 size fractions. Furthermore, there was no clear seasonal pattern of either OP_v or OP levels per μg filter material (OP_m), which agreed with other Mediterranean coastal urban sites in France. The multilinear regression model showed that higher OP levels for PM_{10} in BCN were driven by anthropogenic sources, which were the OC-rich source, Combustion, Heavy Oil, and Road Dust. In contrast, PM_1 was driven by Industry (mostly cement production and a large smelter), which was not a significant source of PM_{10} and $PM_{2.5}$. This shows a possible important health impact of Industry that was not observed when studying PM_{10} and $PM_{2.5}$. For all PM sizes, the levels of OP_m and OP_v were significantly higher in BCN than in MSY, which means that they are mediated by local urban emissions. This is also the cause of the higher levels of OP_v when compared to other stations in France and Switzerland. While most sources were clearly identified, there was no clear OC-rich source in BCN. For this reason, a follow-up study in BCN would be recommended to find all sources of OC-rich PM, and therefore OC, especially in the PM_{10} fraction, as that size fraction had a much higher OP_v than those of $PM_{2.5}$ and PM_1.

In MSY, the levels of OP_m and OP_v were in the same range for PM_{10}, $PM_{2.5}$, and PM_1, meaning that the main source-mediated driver is in the PM_1 fraction, without clear differences in the drivers controlling results for each PM size. Results in MSY were compared to the available results from other stations in France and Switzerland, with MSY having the lowest observed mean OP_v values for PM_{10} and $PM_{2.5}$ from both the DTT and AA assays.

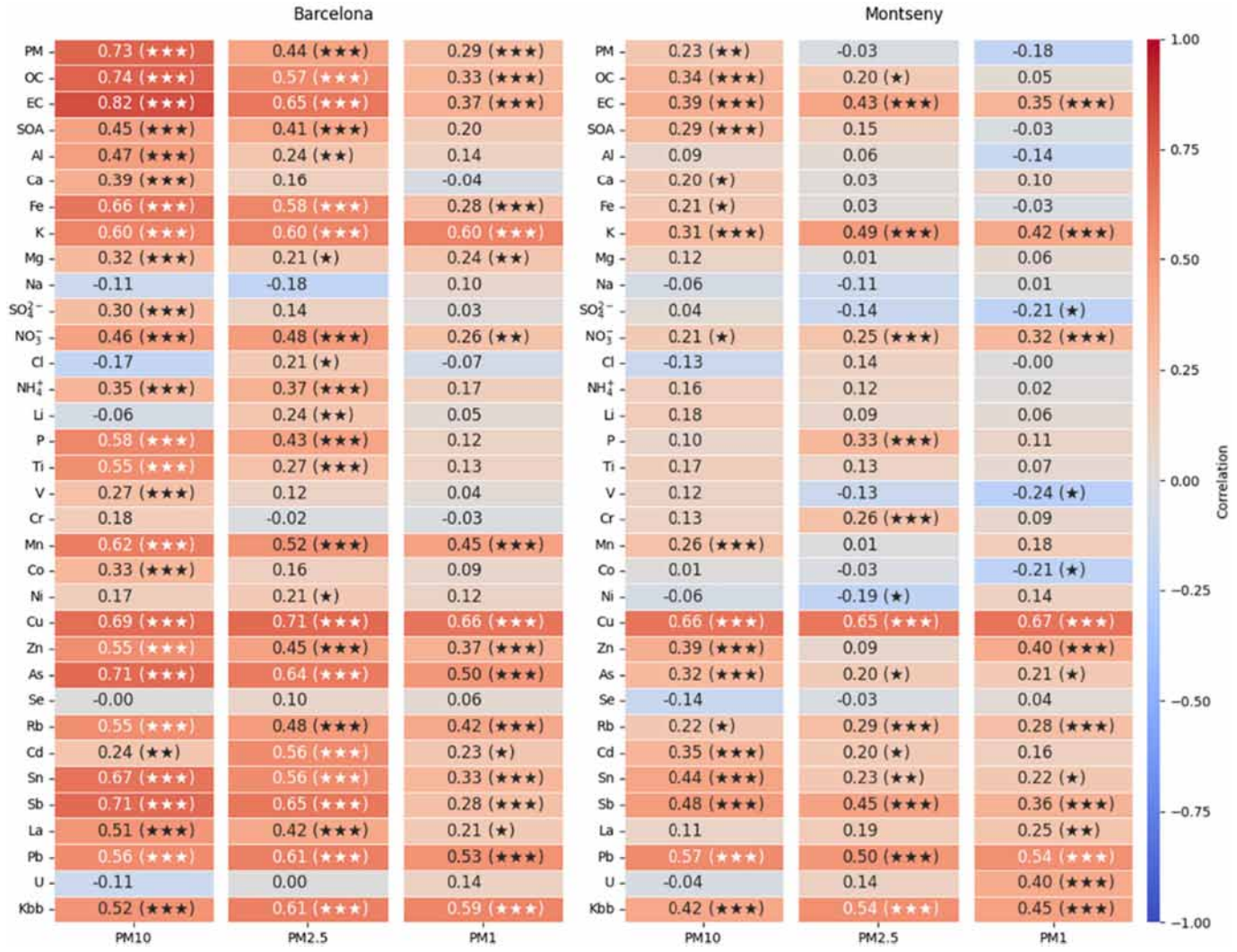

Fig. 5. Pearson's correlation coefficients between OP_v^{AA} and the chemical species for each size of particulate matter (PM) at each site, with statistical significance represented by *** for $p < 0.001$, ** for $p < 0.01$, and * for $p < 0.05$.

Overall, this study indicates that size fraction matters for OP as a function of the environment typology. In an urban context, as already observed in many cities, OP of PM_{10} dominates OP levels, whereas they appear to be governed by PM_1 in rural environments.

Finally, the present study, in addition to previous studies in France and Switzerland, has shown no relation between the PM mass contribution and the OP contribution of each source. Thus, this work also shows the need for epidemiological studies to include OP in their exposure metrics in order to obtain a full picture of how PM affects human health and not to overlook PM_1.

CRediT authorship contribution statement

Marten in 't Veld: Software, Data curation, Formal analysis, Investigation, Writing – original draft, Writing – review & editing, Visualization. **M. Pandolfi:** Software, Validation, Formal analysis. **F. Amato:** Validation. **N. Pérez:** Investigation, Validation. **C. Reche:** Investigation, Validation. **P. Dominutti:** Validation. **J. Jaffrezo:** Validation. **A. Alastuey:** Investigation, Validation. **X. Querol:** Conceptualization, Methodology, Resources, Validation, Investigation, Writing – review & editing, Visualization, Supervision, Project administration, Funding acquisition. **G. Uzu:** Methodology, Investigation, Validation.

Data availability

Data will be made available on request.

Declaration of competing interest

The authors declare that they have no known competing financial interests or personal relationships that could have appeared to influence the work reported in this paper.

Acknowledgements

The present work was supported by the European Union's Horizon 2020 research and innovation program under grant agreement 101036245 (RI-URBANS); the "Agencia Estatal de Investigación" from the Spanish Ministry of Science and Innovation, and FEDER funds under the projects CAIAC (PID2019-108990RB-I00); and the Generalitat de Catalunya (AGAUR 2017 SGR41) and the Direcció General de Territori.

Appendix A. Supplementary data

Supplementary data to this article can be found online at https://doi.org/10.1016/j.scitotenv.2022.159386.

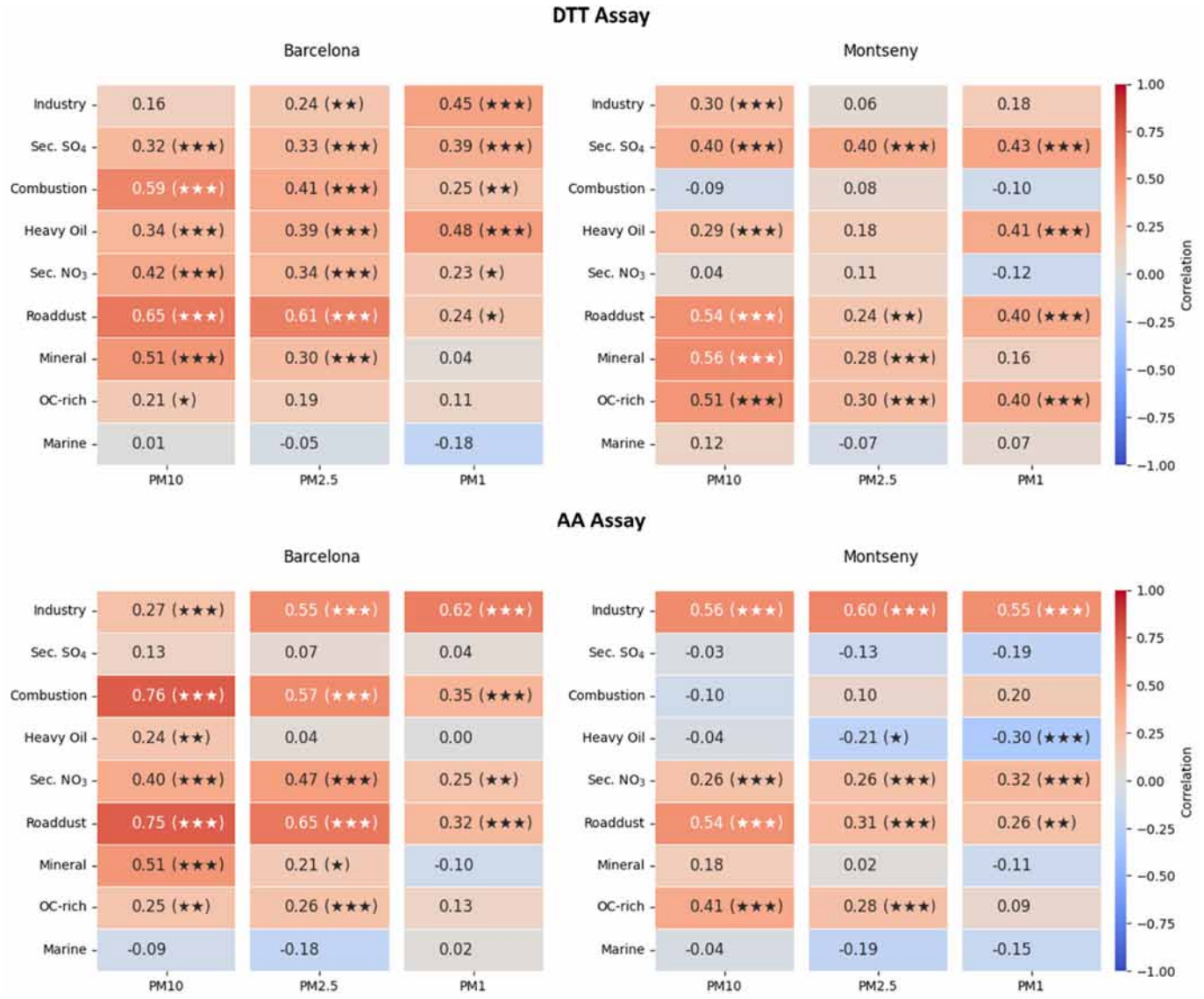

Fig. 6. Pearson's correlation coefficients between Top: OP_v^{DTT} and the sources for each size of particulate matter (PM) at each site, and Bottom: OP_v^{AA} and the sources for each size of PM at each site. The statistical significance is represented by *** for $p < 0.001$, ** for $p < 0.01$, and * for $p < 0.05$.

References

Abbasi, S., Keshavarzi, B., Moore, F., Hopke, P.K., Kelly, F.J., Dominguez, A.O., 2020. Elemental and magnetic analyses, source identification, and oxidative potential of airborne, passive, and street dust particles in Asaluyeh County, Iran. Sci. Total Environ. 707, 136132. https://doi.org/10.1016/j.scitotenv.2019.136132.

Alastuey, A., Minguillón, C., Pérez, N., Querol, X., Viana, M., de Leeuw, F., 2011. The European Topic Centre on Air Pollution and Climate Change Mitigation (ETC/ACM) Is a Consortium of European Institutes Under Contract of the European Environment Agency RIVM UBA-V ÖKO AEAT EMISIA CHMI NILU INERIS PBL CSIC.

Amato, F., Pandolfi, M., Escrig, A., Querol, X., Alastuey, A., Pey, J., Perez, N., Hopke, P.K., 2009a. Quantifying road dust resuspension in urban environment by multilinear engine: a comparison with PMF2. Atmos. Environ. 43, 2770–2780. https://doi.org/10.1016/j.atmosenv.2009.02.039.

Amato, F., Pandolfi, M., Viana, M., Querol, X., Alastuey, A., Moreno, T., 2009b. Spatial and chemical patterns of PM10 in road dust deposited in urban environment. Atmos. Environ. 43, 1650–1659. https://doi.org/10.1016/j.atmosenv.2008.12.009.

Amato, F., Alastuey, A., Karanasiou, A., Lucarelli, F., Nava, S., Calzolai, G., Severi, M., Becagli, S., Gianelle, V.L., Colombi, C., Alves, C., Custódio, D., Nunes, T., Cerqueira, M., Pio, C., Eleftheriadis, K., Diapouli, E., Reche, C., Minguillón, M.C., Manousakas, M.I., Maggos, T., Vratolis, S., Harrison, R.M., Querol, X., 2016. AIRUSE-LIFE+: a harmonized PM speciation and source apportionment in five southern European cities. Atmos. Chem. Phys. 16, 3289–3309. https://doi.org/10.5194/acp-16-3289-2016.

Apte, J.S., Marshall, J.D., Cohen, A.J., Brauer, M., 2015. Addressing global mortality from ambient PM2.5. Environ. Sci. Technol. 49, 8057–8066. https://doi.org/10.1021/acs.est.5b01236.

Bates, J.T., Weber, R.J., Abrams, J., Verma, V., Fang, T., Klein, M., Strickland, M.J., Sarnat, S.E., Chang, H.H., Mulholland, J.A., Tolbert, P.E., Russell, A.G., 2015. Reactive oxygen species generation linked to sources of atmospheric particulate matter and cardiorespiratory effects. Environ. Sci. Technol. 49, 13605–13612. https://doi.org/10.1021/acs.est.5b02967.

Belis, C.A., Larsen, B.R., Amato, F., Haddad, I.el, Favez, O., Harrison, R.M., Hopke, P.K., Nava, S., Paatero, P., Prévôt, A., Quass, U., Vecchi, R., Viana, M., 2014. European Guide on Air Pollution Source Apportionment with Receptor Models, JRC References Report. https://doi.org/10.2788/9307.

Borlaza, L.J.S., Weber, S., Jaffrezo, J.L., Houdier, S., Slama, R., Rieux, C., Albinet, A., Micallef, S., Trébluchon, C., Uzu, G., 2021a. Disparities in particulate matter (PM10) origins and oxidative potential at a city scale (Grenoble, France) - part 2: sources of PM10 oxidative potential using multiple linear regression analysis and the predictive applicability of multilayer perceptron n. Atmos. Chem. Phys. 21, 9719–9739. https://doi.org/10.5194/acp-21-9719-2021.

Borlaza, L.J.S., Weber, S., Marsal, A., Uzu, G., Jacob, V., Besombes, J.L., Chatain, M., Conil, S., Jaffrezo, J.L., 2021b. 9-year trends of PM10 sources and oxidative potential in a rural background site in France. Atmos. Chem. Phys. Discuss. 2021, 1–32.

Boukhenouna, S., Wilson, M.A., Bahmed, K., Kosmider, B., 2018. Reactive oxygen species in chronic obstructive pulmonary disease. Oxidative Med. Cell. Longev. 2018. https://doi.org/10.1155/2018/5730395.

Brines, M., Dall'Osto, M., Amato, F., Minguillón, M.C., Karanasiou, A., Grimalt, J.O., Alastuey, A., Querol, X., van Drooge, B.L., 2019. Source apportionment of urban PM1 in Barcelona during SAPUSS using organic and inorganic components. Environ. Sci. Pollut. Res. 26, 32114–32127. https://doi.org/10.1007/s11356-019-06199-3.

Calas, A., Uzu, G., Kelly, F.J., Houdier, S., Martins, J.M.F., Thomas, F., Molton, F., Charron, A., Dunster, C., Oliete, A., Jacob, V., Besombes, J.L., Chevrier, F., Jaffrezo, J.L., 2018.

Comparison between five acellular oxidative potential measurement assays performed with detailed chemistry on PM10 samples from the city of Chamonix (France). Atmos. Chem. Phys. 18, 7863–7875. https://doi.org/10.5194/acp-18-7863-2018.

Calas, A., Uzu, G., Besombes, J.L., Martins, J.M.F., Redaelli, M., Weber, S., Charron, A., Albinet, A., Chevrier, F., Brulfert, G., Mesbah, B., Favez, O., Jaffrezo, J.L., 2019. Seasonal variations and chemical predictors of oxidative potential (OP) of particulate matter (PM), for seven urban French sites. Atmosphere (Basel) 10, 1–20. https://doi.org/10.3390/atmos10110698.

Castro, L.M., Pio, C.A., Harrison, R.M., Smith, D.J.T., 1999. Carbonaceous aerosol in urban and rural european atmospheres: estimation of secondary organic carbon concentrations. Atmos. Environ. 33, 2771–2781. https://doi.org/10.1016/S1352-2310(98)00331-8.

Cavalli, F., Putaud, J.P., 2010. Toward a Standardized Thermal-optical Protocol for Measuring Atmospheric Organic and Elemental Carbon: The Eusaar Protocol. 48. ACS, Division of Environmental Chemistry - Preprints of Extended Abstracts, pp. 443–446. https://doi.org/10.5194/amtd-2-2321-2009.

Cesari, D., Merico, E., Grasso, F.M., Decesari, S., Belosi, F., Manarini, F., de Nuntiis, P., Rinaldi, M., Volpi, F., Gambaro, A., Morabito, E., Contini, D., 2019. Source apportionment of PM2.5 and of its oxidative potential in an industrial suburban site in South Italy. Atmosphere (Basel) 10. https://doi.org/10.3390/ATMOS10120758.

Chalovich, J.M., Eisenberg, E., 2005. On dithiothreitol (DTT) as a measure of oxidative potential for ambient particles: evidence for the importance of soluble transition metals. Biophys. Chem. 257, 2432–2437. https://doi.org/10.5194/acpd-12-11317-2012.On.

Charrier, J.G., Richards-Henderson, N.K., Bein, K.J., McFall, A.S., Wexler, A.S., Anastasio, C., 2015. Oxidant production from source-oriented particulate matter - part 1: oxidative potential using the dithiothreitol (DTT) assay. Atmos. Chem. Phys. 15, 2327–2340. https://doi.org/10.5194/acp-15-2327-2015.

Chen, L.W.A., Lowenthal, D.H., Watson, J.G., Koracin, D., Kumar, N., Knipping, E.M., Wheeler, N., Craig, K., Reid, S., 2010. Toward effective source apportionment using positive matrix factorization: experiments with simulated PM2.5 data. J. Air Waste Manag. Assoc. 60, 43–54. https://doi.org/10.3155/1047-3289.60.1.43.

Chowdhury, P.H., He, Q., Carmieli, R., Li, C., Rudich, Y., Pardo, M., 2019. Connecting the oxidative potential of secondary organic aerosols with reactive oxygen species in exposed lung cells. Environ. Sci. Technol. 53, 13949–13958. https://doi.org/10.1021/acs.est.9b04449.

Chu, H., Shang, J., Jin, M., Chen, Y., Pan, Y., Li, Y., Tao, X., Cheng, Z., Meng, Q., Li, Q., Jia, G., Zhu, T., Hao, W., Wei, X., 2017. Comparison of lung damage in mice exposed to black carbon particles and 1,4-naphthoquinone coated black carbon particles. Sci. Total Environ. 580, 572–581. https://doi.org/10.1016/j.scitotenv.2016.11.214.

Cohen, A.J., Brauer, M., Burnett, R., Anderson, H.R., Frostad, J., Estep, K., Balakrishnan, K., Brunekreef, B., Dandona, L., Dandona, R., Feigin, V., Freedman, G., Hubbell, B., Jobling, A., Kan, H., Knibbs, L., Liu, Y., Martin, R., Morawska, L., Pope, C.A., Shin, H., Straif, K., Shaddick, G., Thomas, M., van Dingenen, R., van Donkelaar, A., Vos, T., Murray, C.J.L., Forouzanfar, M.H., 2017. Estimates and 25-year trends of the global burden of disease attributable to ambient air pollution: an analysis of data from the Global Burden of Diseases Study 2015. Lancet 389, 1907–1918. https://doi.org/10.1016/S0140-6736(17)30505-6.

Contini, D., Gambaro, A., Belosi, F., de Pieri, S., Cairns, W.R.L., Donateo, A., Zanotto, E., Citron, M., 2011. The direct influence of ship traffic on atmospheric PM 2.5, PM 10 and PAH in Venice. J. Environ. Manag. 92, 2119–2129. https://doi.org/10.1016/j.jenvman.2011.01.016.

Cusack, M., Alastuey, A., Pérez, N., Pey, J., Querol, X., 2012. Trends of particulate matter (PM 2.5) and chemical composition at a regional background site in the Western Mediterranean over the last nine years (2002–2010). Atmos. Chem. Phys. 12, 8341–8357. https://doi.org/10.5194/acp-12-8341-2012.

Daellenbach, K.R., Uzu, G., Jiang, J., Cassagnes, L.-E., Leni, Z., Vlachou, A., Stefenelli, G., Canonaco, F., Weber, S., Segers, A., Kuenen, J.J.P., Schaap, M., Favez, O., Albinet, A., Aksoyoglu, S., Dommen, J., Baltensperger, U., Geiser, M., el Haddad, I., Jaffrezo, J.-L., Prévôt, A.S.H., 2020. Sources of particulate-matter air pollution and its oxidative potential in Europe. Nature 587, 414–419. https://doi.org/10.1038/s41586-020-2902-8.

Decesari, S., Sowlat, M.H., Hasheminassab, S., Sandrini, S., Gilardoni, S., Facchini, M.C., Fuzzi, S., Sioutas, C., 2017. Enhanced toxicity of aerosol in fog conditions in the Po Valley, Italy. Atmos. Chem. Phys. 17, 7721–7731. https://doi.org/10.5194/acp-17-7721-2017.

Delfino, R.J., Staimer, N., Tjoa, T., Arhami, M., Polidori, A., Gillen, D.L., George, S.C., Shafer, M.M., Schauer, J.J., Sioutas, C., 2010. Associations of primary and secondary organic aerosols with airway and systemic inflammation in an elderly panel cohort. Epidemiology 21, 892–902. https://doi.org/10.1097/EDE.0b013e3181f20e6c.

Demographia World Urban Areas, 2020. Demographia World Urban Areas, 16th Annual Edition 2020.06. 25. Demographia.

Dinoi, A., Cesari, D., Marinoni, A., Bonasoni, P., Riccio, A., Chianese, E., Tirimberio, G., Naccarato, A., Sprovieri, F., Andreoli, V., Moretti, S., Gullì, D., Calidonna, C.R., Ammoscato, I., Contini, D., 2017. Inter-comparison of carbon content in PM2.5 and PM10 collected at five measurement sites in Southern Italy. Atmosphere (Basel) 8. https://doi.org/10.3390/atmos8120243.

Escrig Vidal, A., Monfort, E., Celades, I., Querol, X., Amato, F., Minguillón, M.C., Hopke, P.K., 2009. Application of optimally scaled target factor analysis for assessing source contribution of ambient PM10. J. Air Waste Manag. Assoc. 59, 1296–1307. https://doi.org/10.3155/1047-3289.59.11.1296.

Gangwar, R.S., Bevan, G.H., Palanivel, R., Das, L., Rajagopalan, S., 2020. Oxidative stress pathways of air pollution mediated toxicity: recent insights. Redox Biol. 34, 101545. https://doi.org/10.1016/j.redox.2020.101545.

Grange, S.K., Uzu, G., Weber, S., Jaffrezo, J., Hueglin, C., 2022. Linking Switzerland's PM10 and PM2.5 Oxidative Potential (OP) With Emission Sources, pp. 1–31. https://doi.org/10.5194/acp-2021-979.

Gulliver, J., Morley, D., Dunster, C., McCrea, A., van Nunen, E., Tsai, M.Y., Probst-Hensch, N., Eeftens, M., Imboden, M., Ducret-Stich, R., Naccarati, A., Galassi, C., Ranzi, A., Nieuwenhuijsen, M., Curto, A., Donaire-Gonzalez, D., Cirach, M., Vermeulen, R., Vineis, P., Hoek, G., Kelly, F.J., 2018. Land use regression models for the oxidative potential of fine particles (PM2.5) in five European areas. Environ. Res. 160, 247–255. https://doi.org/10.1016/j.envres.2017.10.002.

Hime, N.J., Marks, G.B., Cowie, C.T., 2018. A comparison of the health effects of ambient particulate matter air pollution from five emission sources. Int. J. Environ. Res. Public Health 15, 1–24. https://doi.org/10.3390/ijerph15061206.

Hopke, P.K., Hidy, G., 2022. Changing emissions results in changed PM2.5 composition and health impacts. Atmosphere (Basel) 13, 193. https://doi.org/10.3390/atmos13020193.

in 't Veld, M., Alastuey, A., Pandolfi, M., Amato, F., Pérez, N., Reche, C., Via, M., Minguillón, M.C., Escudero, M., Querol, X., 2021. Compositional changes of PM2.5 in NE Spain during 2009–2018: a trend analysis of the chemical composition and source apportionment. Sci. Total Environ. 795. https://doi.org/10.1016/j.scitotenv.2021.148728.

Jacob, D.J., 1999. CHAPTER 8: aerosols. Introduction to Atmospheric Chemistry. Princeton University Press, pp. 144–152. https://doi.org/10.1111/j.0954-6820.1949.tb11329.x.

Janssen, N.A.H., Yang, A., Strak, M., Steenhof, M., Hellack, B., Gerlofs-Nijland, M.E., Kuhlbusch, T., Kelly, F., Harrison, R., Brunekreef, B., Hoek, G., Cassee, F., 2014. Oxidative potential of particulate matter collected at sites with different source characteristics. Sci. Total Environ. 472, 572–581. https://doi.org/10.1016/j.scitotenv.2013.11.099.

Jia, Y.Y., Wang, Q., Liu, T., 2017. Toxicity research of PM2.5 compositions in vitro. Int. J. Environ. Res. Public Health 14. https://doi.org/10.3390/ijerph14030232.

Kelly, F.J., Fussell, J.C., 2012. Size, source and chemical composition as determinants of toxicity attributable to ambient particulate matter. Atmos. Environ. 60, 504–526. https://doi.org/10.1016/j.atmosenv.2012.06.039.

Lelieveld, J., Evans, J.S., Fnais, M., Giannadaki, D., Pozzer, A., 2015. The contribution of outdoor air pollution sources to premature mortality on a global scale. Nature 525, 367–371.

Lelieveld, J., Pozzer, A., Pöschl, U., Fnais, M., Haines, A., Münzel, T., 2020. Loss of life expectancy from air pollution compared to other risk factors: a worldwide perspective. Cardiovasc. Res. 116, 1910–1917. https://doi.org/10.1093/cvr/cvaa025.

Li, N., Xia, T., Nel, A.E., 2008. The role of oxidative stress in ambient particulate matter- induced lung diseases and its implications in the toxicity of engineered nanoparticles. Free Rad. Biol. Med. 44, 1689–1699. https://doi.org/10.1016/j.freeradbiomed.2008.01.028.The.

Li, Q., Shang, J., Zhu, T., 2013. Physicochemical characteristics and toxic effects of ozone-oxidized black carbon particles. Atmos. Environ. 81, 68–75. https://doi.org/10.1016/j.atmosenv.2013.08.043.

Li, J., Chen, H., Li, X., Wang, M., Zhang, X., Cao, J., Shen, F., Wu, Y., Xu, S., Fan, H., Da, G., Huang, R.jin, Wang, J., Chan, C.K., de Jesus, A.L., Morawska, L., Yao, M., 2019. Differing toxicity of ambient particulate matter (PM)in global cities. Atmos. Environ. 212, 305–315. https://doi.org/10.1016/j.atmosenv.2019.05.048.

Liu, X., Chen, Z., 2017. The pathophysiological role of mitochondrial oxidative stress in lung diseases. J. Transl. Med. 15, 1–13. https://doi.org/10.1186/s12967-017-1306-5.

Minguillón, M.C., Perron, N., Querol, X., Szidat, S., Fahrni, S.M., Alastuey, A., Jimenez, J.L., Mohr, C., Ortega, A.M., Day, D.A., Lanz, V.A., Wacker, L., Reche, C., Cusack, M., Amato, F., Kiss, G., Hoffer, A., Decesari, S., Moretti, F., Hillamo, R., Teinilä, K., Seco, R., Peñuelas, J., Metzger, A., Schallhart, S., Müller, M., Hansel, A., Burkhart, J.F., Baltensperger, U., Prévót, A.S.H., 2011. Fossil versus contemporary sources of fine elemental and organic carbonaceous particulate matter during the DAURE campaign in Northeast Spain. Atmos. Chem. Phys. 11, 12067–12084. https://doi.org/10.5194/acp-11-12067-2011.

Mohammed, G., Karani, G., Mitchell, D., 2017. Trace elemental composition in PM10 and PM2.5 collected in Cardiff, Wales. Energy Procedia 111, 540–547. https://doi.org/10.1016/j.egypro.2017.03.216.

Mohr, C., DeCarlo, P.F., Heringa, M.F., Chirico, R., Slowik, J.G., Richter, R., Reche, C., Alastuey, A., Querol, X., Seco, R., Peñuelas, J., Jiménez, J.L., Crippa, M., Zimmermann, R., Baltensperger, U., Prévot, A.S.H., 2012. Identification and quantification of organic aerosol from cooking and other sources in Barcelona using aerosol mass spectrometer data. Atmos. Chem. Phys. 12, 1649–1665. https://doi.org/10.5194/acp-12-1649-2012.

Moldanová, J., Fridell, E., Popovicheva, O., Demirdjian, B., Tishkova, V., Faccinetto, A., Focsa, C., 2009. Characterisation of particulate matter and gaseous emissions from a large ship diesel engine. Atmos. Environ. 43, 2632–2641. https://doi.org/10.1016/j.atmosenv.2009.02.008.

Moreno, T., Querol, X., Alastuey, A., Viana, M., Salvador, P., Sánchez de la Campa, A., Artiñano, B., de la Rosa, J., Gibbons, W., 2006. Variations in atmospheric PM trace metal content in Spanish towns: illustrating the chemical complexity of the inorganic urban aerosol cocktail. Atmos. Environ. 40, 6791–6803. https://doi.org/10.1016/j.atmosenv.2006.05.074.

Moreno, T., Querol, X., Alastuey, A., Reche, C., Cusack, M., Amato, F., Pandolfi, M., Pey, J., Richard, A., Prévôt, A.S.H., Furger, M., Gibbons, W., 2011. Variations in time and space of trace metal aerosol concentrations in urban areas and their surroundings. Atmos. Chem. Phys. 11, 9415–9430. https://doi.org/10.5194/acp-11-9415-2011.

Moufarrej, L., Courcot, D., Ledoux, F., 2020. Assessment of the PM2.5 oxidative potential in a coastal industrial city in Northern France: relationships with chemical composition, local emissions and long range sources. Sci. Total Environ. 748, 141448. https://doi.org/10.1016/j.scitotenv.2020.141448.

Naraki, H., Keshavarzi, B., Zarei, M., Moore, F., Abbasi, S., Kelly, F.J., Dominguez, A.O., Jaafarzadeh, N., 2021. Urban street dust in the Middle East oldest oil refinery zone: oxidative potential, source apportionment,and health risk assessment of potentially toxic elements. Chemosphere 268, 128825. https://doi.org/10.1016/j.chemosphere.2020.128825.

Nelin, T.D., Joseph, A.M., Gorr, M.W., Wold, L.E., 2012. Direct and indirect effects of PM on the cardiovascular system. Toxicol. Lett. 208, 293–299. https://doi.org/10.1016/j.toxlet.2011.11.008.Direct.

Niranjan, R., Thakur, A.K., 2017. The toxicological mechanisms of environmental soot (black carbon) and carbon black: focus on oxidative stress and inflammatory pathways. Front. Immunol. https://doi.org/10.3389/fimmu.2017.00763.

Norris, G., Duvall, R., Brown, S., Bai, S., 2014. EPA Positive Matrix Factorization (PMF) 5.0 Fundamentals and User Guide [WWW Document]. EPA.
Paatero, P., Tapper, U., 1994. Positive matrix factorization: a non-negative factor model with optimal utilization of error estimates of data values. Environmetrics 5, 111–126.
Pachon, J.E., Weber, R.J., Zhang, X., Mulholland, J.A., Russell, A.G., 2013. Revising the use of potassium (K) in the source apportionment of PM2.5. Atmos. Pollut. Res. 4, 14–21. https://doi.org/10.5094/APR.2013.002.
Pandolfi, M., Gonzalez-Castanedo, Y., Alastuey, A., de la Rosa, J.D., Mantilla, E., de la Campa, A.S., Querol, X., Pey, J., Amato, F., Moreno, T., 2011. Source apportionment of PM10 and PM2.5 at multiple sites in the strait of Gibraltar by PMF: impact of shipping emissions. Environ. Sci. Pollut. Res. 18, 260–269. https://doi.org/10.1007/s11356-010-0373-4.
Pandolfi, M., Amato, F., Reche, C., Alastuey, A., Otjes, R.P., Blom, M.J., Querol, X., 2012. Summer ammonia measurements in a densely populated Mediterranean city. Atmos. Chem. Phys. 12, 7557–7575. https://doi.org/10.5194/acp-12-7557-2012.
Pandolfi, M., Querol, X., Alastuey, A., Jimenez, J.L., Jorba, O., Day, D., Ortega, A., Cubison, M.J., Comerón, A., Sicard, M., Mohr, C., Prevot, A.S.H., Minguillón, M.C., Pey, J., Baldasano, J.M., Burkhart, J.F., Seco, R., Peñuelas, J., van Drooge, B.L., Artiñano, B., di Marco, C., Nemitz, E., Schallhart, S., Metzger, A., Hansel, A., Lorente, J., Ng, S., Jayne, J., Szidat, S., 2014. Effects of sources and meteorology on particulate matter in the Western Mediterranean Basin: an overview of the DAURE campaign. J. Geophys. Res. 119, 4978–5010. https://doi.org/10.1002/2013JD021079.
Pandolfi, M., Alastuey, A., Pérez, N., Reche, C., Castro, I., Shatalov, V., Querol, X., 2016. Trends analysis of PM source contributions and chemical tracers in NE Spain during 2004–2014: a multi-exponential approach. Atmos. Chem. Phys. 16, 11787–11805. https://doi.org/10.5194/acp-16-11787-2016.
Pandolfi, M., Mooibroek, D., Hopke, P., van Pinxteren, D., Querol, X., Herrmann, H., Alastuey, A., Favez, O., Hüglin, C., Perdrix, E., Riffault, V., Sauvage, S., van der Swaluw, E., Tarasova, O., Colette, A., 2020. Long range and local air pollution: what can we learn from chemical speciation of particulate matter at paired sites? Atmos. Chem. Phys. Discuss. 20, 409–429. https://doi.org/10.5194/acp-2019-493.
Park, H.S., Kim, S.R., Lee, Y.C., 2009. Impact of oxidative stress on lung diseases. Respirology 14, 27–38. https://doi.org/10.1111/j.1440-1843.2008.01447.x.
Park, M., Joo, H.S., Lee, K., Jang, M., Kim, S.D., Kim, I., Borlaza, L.J.S., Lim, H., Shin, H., Chung, K.H., Choi, Y.H., Park, S.G., Bae, M.S., Lee, J., Song, H., Park, K., 2018. Differential toxicities of fine particulate matters from various sources. Sci. Rep. 8, 1–11. https://doi.org/10.1038/s41598-018-35398-0.
Pérez, N., Pey, J., Castillo, S., Viana, M., Alastuey, A., Querol, X., 2008. Interpretation of the variability of levels of regional background aerosols in the Western Mediterranean. Sci. Total Environ. 407, 527–540. https://doi.org/10.1016/j.scitotenv.2008.09.006.
Pérez, N., Pey, J., Reche, C., Cortés, J., Alastuey, A., Querol, X., 2016. Impact of harbour emissions on ambient PM10 and PM2.5 in Barcelona (Spain): evidences of secondary aerosol formation within the urban area. Sci. Total Environ. 571, 237–250. https://doi.org/10.1016/j.scitotenv.2016.07.025.
Pernigotti, D., Belis, C.A., 2018. DeltaSA tool for source apportionment benchmarking, description and sensitivity analysis. Atmos. Environ. 180, 138–148. https://doi.org/10.1016/j.atmosenv.2018.02.046.
Perrone, M.R., Bertoli, I., Romano, S., Russo, M., Rispoli, G., Pietrogrande, M.C., 2019. PM2.5 and PM10 oxidative potential at a Central Mediterranean Site: contrasts between dithiothreitol- and ascorbic acid-measured values in relation with particle size and chemical composition. Atmos. Environ. 210, 143–155. https://doi.org/10.1016/j.atmosenv.2019.04.047.
Pey, J., Querol, X., Alastuey, A., 2009. Variations of levels and composition of PM10 and PM2.5 at an insular site in the Western Mediterranean. Atmos. Res. 94, 285–299. https://doi.org/10.1016/j.atmosres.2009.06.006.
Querol, X., Alastuey, A., Rodriguez, S., Plana, F., Ruiz, C.R., Cots, N., Massagué, G., Puig, O., 2001. PM10 and PM2.5 source apportionment in the Barcelona Metropolitan area, Catalonia, Spain. Atmos. Environ. 35, 6407–6419. https://doi.org/10.1016/S1352-2310(01)00361-2.
Querol, X., Alastuey, A., Ruiz, C.R., Artiñano, B., Hansson, H.C., Harrison, R.M., Buringh, E., ten Brink, H.M., Lutz, M., Bruckmann, P., Straehl, P., Schneider, J., 2004a. Speciation and origin of PM10 and PM2.5 in selected European cities. Atmos. Environ. 38, 6547–6555. https://doi.org/10.1016/j.atmosenv.2004.08.037.
Querol, X., Alastuey, A., Viana, M.M., Rodriguez, S., Artiñano, B., Salvador, P., Garcia Do Santos, S., Fernandez Patier, R., Ruiz, C.R., de La Rosa, J., Sanchez De La Campa, A., Menendez, M., Gil, J.I., 2004. Speciation and origin of PM10 and PM2.5 in Spain. J. Aerosol Sci. 35, 1151–1172. https://doi.org/10.1016/j.jaerosci.2004.04.002.
Querol, X., Alastuey, A., Moreno, T., Viana, M.M., Castillo, S., Pey, J., Rodríguez, S., Cristóbal, A., Jiménez, S., Pallarés, M., de la Rosa, J., Artíñano, B., Salvador, P., Sánchez, M., García Dos Santos, S., Herce Garraleta, M.D., Fernández-Patier, R., Moreno-Grau, S., Negral, L., Minguillón, M.C., Monfort, E., Sanz, M.J., Palomo-Marín, R., Pinilla-Gil, E., Cuevas, E., 2006. Atmospheric Particulate Matter in Spain: Levels, Composition and Source Origin 80.
Querol, X., Viana, M., Alastuey, A., Amato, F., Moreno, T., Castillo, S., Pey, J., de la Rosa, J., Sánchez de la Campa, A., Artíñano, B., Salvador, P., García Dos Santos, S., Fernández-Patier, R., Moreno-Grau, S., Negral, L., Minguillón, M.C., Monfort, E., Gil, J.I., Inza, A., Ortega, L.A., Santamaría, J.M., Zabalza, J., 2007. Source origin of trace elements in PM from regional background, urban and industrial sites of Spain. Atmos. Environ. 41, 7219–7231. https://doi.org/10.1016/j.atmosenv.2007.05.022.
Querol, X., Alastuey, A., Pandolfi, M., Reche, C., Pérez, N., Minguillón, M.C., Moreno, T., Viana, M., Escudero, M., Orio, A., Pallarés, M., Reina, F., 2014. 2001–2012 trends on air quality in Spain. Sci. Total Environ. 490, 957–969. https://doi.org/10.1016/j.scitotenv.2014.05.074.
Reche, C., Viana, M., Amato, F., Alastuey, A., Moreno, T., Hillamo, R., Teinilä, K., Saarnio, K., Seco, R., Peñuelas, J., Mohr, C., Prévôt, A.S.H., Querol, X., 2012. Biomass burning contributions to urban aerosols in a coastal Mediterranean City. Sci. Total Environ. 427–428, 175–190. https://doi.org/10.1016/j.scitotenv.2012.04.012.
Reff, A., Eberly, S.I., Bhave, P.V., 2007. Receptor modeling of ambient particulate matter data using positive matrix factorization: review of existing methods. J. Air Waste Manag. Assoc. 57, 146–154. https://doi.org/10.1080/10473289.2007.10465319.
Ripoll, A., Minguillón, M.C., Pey, J., Pérez, N., Querol, X., Alastuey, A., 2015. Joint analysis of continental and regional background environments in the western Mediterranean: PM1 and PM10 concentrations and composition. Atmos. Chem. Phys. 15, 1129–1145. https://doi.org/10.5194/acp-15-1129-2015.
Rosanna, D.P., Salvatore, C., 2012. Reactive oxygen species, inflammation, and lung diseases. Curr. Pharm. Des. 18, 3889–3900. https://doi.org/10.2174/138161212802083716.
Scerri, M.M., Genga, A., Iacobellis, S., Delmaire, G., Giove, A., Siciliano, M., Siciliano, T., Weinbruch, S., 2019. Investigating the plausibility of a PMF source apportionment solution derived using a small dataset: a case study from a receptor in a rural site in Apulia - South East Italy. Chemosphere 236, 124376. https://doi.org/10.1016/j.chemosphere.2019.124376.
Seabold, S., Perktold, J., 2010. Statsmodels: econometric and statistical modeling with Python. Proceedings of the 9th Python in Science Conference, pp. 92–96. https://doi.org/10.25080/majora-92bf1922-011.
Trechera, P., Moreno, T., Córdoba, P., Moreno, N., Amato, F., Cortés, J., Zhuang, X., Li, B., Li, J., Shangguan, Y., Dominguez, A.O., Kelly, F., Mhadhbi, T., Jaffrezo, J.L., Uzu, G., Querol, X., 2021. Geochemistry and oxidative potential of the respirable fraction of powdered mined Chinese coals. Sci. Total Environ. 800, 149486. https://doi.org/10.1016/j.scitotenv.2021.149486.
Turpin, B.J., Huntzicker, J.J., 1995. Identification of secondary organic aerosol episodes and quantitation of primary and secondary organic aerosol concentrations during SCAQS. Atmos. Environ. 29, 3527–3544. https://doi.org/10.1016/1352-2310(94)00276-Q.
Turpin, B.J., Lim, H.J., 2001. Species contributions to pm2.5 mass concentrations: revisiting common assumptions for estimating organic mass. Aerosol Sci. Technol. 35, 602–610. https://doi.org/10.1080/02786820119445.
Turpin, B.J., Saxena, P., Allen, G., Koutrakis, P., McMurry, P., Hildemann, L., 1997. Characterization of the southwestern desert aerosol, Meadview, AZ. J. Air Waste Manag. Assoc. 47, 344–356. https://doi.org/10.1080/10473289.1997.10464451.
Viana, M., Reche, C., Amato, F., Alastuey, A., Querol, X., Moreno, T., Lucarelli, F., Nava, S., Calzolai, G., Chiari, M., Rico, M., 2013. Evidence of biomass burning aerosols in the Barcelona urban environment during winter time. Atmos. Environ. 72, 81–88. https://doi.org/10.1016/j.atmosenv.2013.02.031.
Viana, M., Hammingh, P., Colette, A., Querol, X., Degraeuwe, B., de Vlieger, I., van Aardenne, J., 2014. Impact of maritime transport emissions on coastal air quality in Europe. Atmos. Environ. 90, 96–105. https://doi.org/10.1016/j.atmosenv.2014.03.046.
Wang, X., Bi, X., Sheng, G., Fu, J., 2006. Chemical composition and sources of PM10 and PM2.5 aerosols in Guangzhou,China. Environ. Monit. Assess. 119, 425–439. https://doi.org/10.1007/s10661-005-9034-3.
Wang, S., Ye, J., Soong, R., Wu, B., Yu, L., Simpson, A.J., Chan, A.W.H., 2018. Relationship between chemical composition and oxidative potential of secondary organic aerosol from polycyclic aromatic hydrocarbons. Atmos. Chem. Phys. 18, 3987–4003. https://doi.org/10.5194/acp-18-3987-2018.
Weber, S., Uzu, G., Calas, A., Chevrier, F., Besombes, J.L., Charron, A., Salameh, D., Ježek, I., Močnik, G., Jaffrezo, J.L., 2018. An apportionment method for the oxidative potential of atmospheric particulate matter sources: application to a one-year study in Chamonix, France. Atmos. Chem. Phys. 18, 9617–9629. https://doi.org/10.5194/acp-18-9617-2018.
Weber, S., Salameh, D., Albinet, A., Alleman, L.Y., Waked, A., Besombes, J.L., Jacob, V., Guillaud, G., Meshbah, B., Rocq, B., Hulin, A., Dominik-Sègue, M., Chrétien, E., Jaffrezo, J.L., Favez, O., 2019. Comparison of PM10 sources profiles at 15 French sites using a harmonized constrained positive matrix factorization approach. Atmosphere (Basel) 10, 1–22. https://doi.org/10.3390/atmos10060310.
Weber, S., Uzu, G., Favez, O., Borlaza, L.J.S., Calas, A., Salameh, D., Chevrier, F., Allard, J., Besombes, J.L., Albinet, A., Pontet, S., Mesbah, B., Gille, G., Zhang, S., Pallares, C., Leoz-Garziandia, E., Jaffrezo, J.L., 2021. Source apportionment of atmospheric PM10 oxidative potential: synthesis of 15 year-round urban datasets in France. Atmos. Chem. Phys. 21, 11353–11378. https://doi.org/10.5194/acp-21-11353-2021.
Weichenthal, S., Lavigne, E., Evans, G., Pollitt, K., Burnett, R.T., 2016. Ambient PM2.5 and risk of emergency room visits for myocardial infarction: impact of regional PM2.5 oxidative potential: a case-crossover study. Environ. Health 15, 1–9. https://doi.org/10.1186/s12940-016-0129-9.
WHO, 2006. WHO Air Quality Guidelines for Particulate Matter, Ozone, Nitrogen Dioxide and Sulfur Dioxide: Global Update 2005: Summary of Risk Assessment. World Health Organization.
WHO, 2013. Review of Evidence on Health Aspects of Air Pollution - REVIHAAP Project. https://doi.org/10.1007/BF00379640.
WHO, 2016. Ambient Air Pollution: A Global Assessment of Exposure and Burden of Disease. World Health Organization.
WHO, 2018. Burden of Disease From Ambient Air Pollution for 2016.
WHO, 2021. WHO Global Air Quality Guidelines 2021. World Health Organization.
WHO, 2021. WHO "Global Air Quality Guidelines" Organization.
Wu, C., Yu, J.Z., 2016. Determination of primary combustion source organic carbon-to-elemental carbon (OC/EC) ratio using ambient OC and EC measurements: secondary OC-EC correlation minimization method. Atmos. Chem. Phys. 16, 5453–5465. https://doi.org/10.5194/acp-16-5453-2016.
Yang, A., Jedynska, A., Hellack, B., Kooter, I., Hoek, G., Brunekreef, B., Kuhlbusch, T.A.J., Cassee, F.R., Janssen, N.A.H., 2014. Measurement of the oxidative potential of PM2.5 and its constituents: the effect of extraction solvent and filter type. Atmos. Environ. 83, 35–42. https://doi.org/10.1016/j.atmosenv.2013.10.049.
Yu, S., Dennis, R.L., Bhave, P.V., Eder, B.K., 2004. Primary and secondary organic aerosols over the United States: estimates on the basis of observed organic carbon (OC) and elemental carbon (EC), and air quality modeled primary OC/EC ratios. Atmos Environ 38, 5257–5268. https://doi.org/10.1016/j.atmosenv.2004.02.064.

Yu, J., Yan, C., Liu, Y., Li, X., Zhou, T., Zheng, M., 2018. Potassium: a tracer for biomass burning in Beijing? Aerosol Air Qual. Res. 18, 2447–2459. https://doi.org/10.4209/aaqr.2017.11.0536.

Zhang, H., Li, Z., Liu, Y., Xinag, P., Cui, X.Y., Ye, H., Hu, B.L., Lou, L.P., 2018. Physical and chemical characteristics of PM2.5 and its toxicity to human bronchial cells BEAS-2B in the winter and summer. J. Zhejiang Univ. Sci. B 19, 317–326. https://doi.org/10.1631/jzus.B1700123.

Zhang, W., Lin, S., Hopke, P.K., Thurston, S.W., van Wijngaarden, E., Croft, D., Squizzato, S., Masiol, M., Rich, D.Q., 2018. Triggering of cardiovascular hospital admissions by fine particle concentrations in New York state: before, during, and after implementation of multiple environmental policies and a recession. Environ. Pollut. 242, 1404–1416. https://doi.org/10.1016/j.envpol.2018.08.030.